



# Geoheritage in a Mythical and Volcanic Terrain: an Inventory and Assessment Study for Geopark and Geotourism, Nemrut Volcano (Bitlis, Eastern Turkey)

Can Ertekin<sup>1,2</sup> · Yunus Levent Ekinci<sup>3,4</sup> · Aydın Büyüksaraç<sup>5</sup> · Rezzan Ekinci<sup>6</sup>

Received: 13 August 2020 / Accepted: 18 June 2021

© The European Association for Conservation of the Geological Heritage 2021

## Abstract

Mt. Nemrut (Nemrut volcano or caldera) is a quiescent Quaternary volcano situated in Eastern Anatolia (Turkey) near the western shore of Lake Van. The onset of Nemrut volcanism comprised lava flows and the formation of peripheral silicic doming representing the pre-caldera stage. After the syn-caldera stage (caldera-forming), which entailed widespread pyroclastics, the post-caldera stage produced peralkaline-type rocks, ash eruptions, and rift activities with basalt- and rhyolite (comendite)-type lava flows; a lava lake represents the latest volcanic activity (1441, 1597, and 1692 AD). The scope of this study involves building an inventory and assessing the site-specific geodiversity elements of Nemrut volcano that are relevant for geotourism use and geopark development. Nemrut volcano produces diverse abiotic elements with geomorphologic, structural, lithologic, and hydrologic values. The domes (Kirkor and Kale) and the Nemrut camels are geomorphological geosites. The lakes (hot and cold lakes) are hydrological geosites. The rift zone includes geosites with lithologic elements. The Nemrut caldera geosite consists of different amalgamations of abiotic elements. The method of Brilha (2016) was used to assess the geosites of Nemrut volcano. The average *scientific value* and geotourism use (*potential touristic use*) scores for all geosites are 3.16 and 2.32, respectively. The *scientific values* are greatest for the geosites of the caldera (3.60) and the lakes (3.40). The highest geotourism scores match well with the highest *scientific value* scores, obtained for the caldera and the lakes. The geological diversity indicator, a sub-component of the *scientific value*, is remarkably high for the caldera geosite (0.2) compared to the other geosites (0.0). The *uniqueness* (a geo-patrimonial criterion), bio-cultural and aesthetic scores highly influence the geotourism scores for the geosites of the caldera, lakes and rift zone compared to the scores of the other geosites. We propose that Nemrut volcano, and especially the geosites of Nemrut caldera and the lakes, has significant geopark and geoheritage values. Nemrut volcano, a proposed geopark site, exhibits the most recent volcanism in Anatolia and is among the geoparks included in the European Geoparks Network. The volcano is registered as a Ramsar site and supports vulnerable and endangered species (*Melanitta fusca* and endemic plants). The volcano is also a distinctive cultural landscape with a mythical origin and is relatively close to the touristic sites of the ruins of Urartu, an archaic kingdom in the northern part of the ancient Near East extending into portions of Eastern Anatolia. Due to these cultural assets and geo-assets, Nemrut volcano is a relevant geotouristic destination. The development of this volcano into a geopark may contribute to rural development by increasing local gross domestic product (GDP) in terms of employment and touristic traffic. Additionally, we make some recommendations related to infrastructure, precautions (medical services and a warning system for natural hazards), tourism services and a geopark tourist route to increase the importance of the volcano as a geopark.

✉ Can Ertekin  
can\_ertekin@yahoo.com

<sup>1</sup> Aegean Regional Directorate of Mineral Research and Exploration, İzmir, Turkey

<sup>2</sup> Graduate School of Natural and Applied Sciences, Geology Engineering Department, Çanakkale Onsekiz Mart University, Çanakkale, Turkey

<sup>3</sup> Bitlis Eren University, Faculty of Arts and Sciences, Department of Art History, Bitlis, Turkey

<sup>4</sup> Career Application and Research Centre, Bitlis Eren University, Bitlis, Turkey

<sup>5</sup> Çanakkale Onsekiz Mart University, Çan Vocational School, Çanakkale, Çan, Turkey

<sup>6</sup> Geophysical Engineer, Bitlis, Turkey

**Keywords** Geosite · Geotourism · Geopark · Parameterization · Nemrut caldera · Eastern Anatolia · Turkey

## Introduction

Eastern Anatolia, the eastern part of Turkey, is a geographic region covered by volcanic provinces (Fig. 1). Volcanism is represented by major Quaternary volcanic centres (e.g. Nemrut volcano in Fig. 2). Nemrut volcano (a stratovolcano) or Nemrut caldera was active in historical times (1441, 1597, and 1692 AD). Its activity is also indicated in historical records (chronological activity list in Ulusoy et al. 2012). In addition, the eruptions, rift lava flows, and activity of the caldera in the historical period can be linked with historical events associated with the mythical forms of the King of Nemruz. Eastern Anatolia is a virgin territory for geoheritage-geodiversity-geopark studies despite the historical, volcanic and mythic background of the region. Inventory studies conducted for geosite selections are mainly carried out for the western-central parts of Turkey (Fig. 1). In addition, geopark studies in Turkey are also comparatively new, according to European geopark experience.

The geoparks located throughout Europe serve economic development; this is defined as geotourism, in which features of Earth's elements are used sustainably as touristic resources to attract tourists and share geoscientific knowledge (Chen et al. 2015; EGN 2020). Geoparks in Europe are organized under the European Geoparks Network (EGN). The EGN consists of numerous geosites that must be part of the local geological heritage and may include cultural assets (EGN 2020). Unlike the European perspective, natural regulations regarding geodiversity are not well-defined outside of Europe (de Lima et al. 2010; Çetiner et al. 2018). In Turkey, site descriptions are classified into archaeological sites, cultural-natural assets, sites of ecological value, wetlands, national parks, natural parks, and natural monuments. Hence, comprehensive legislation can be considered a juxtaposition of two phases of management: conservation and biological protection (Çetiner et al. 2018). The relevant legislation in Turkey is not sufficient to categorize or inventory features of geodiversity. Consequently, Turkey has not fully progressed towards the conservation (monument-designating and

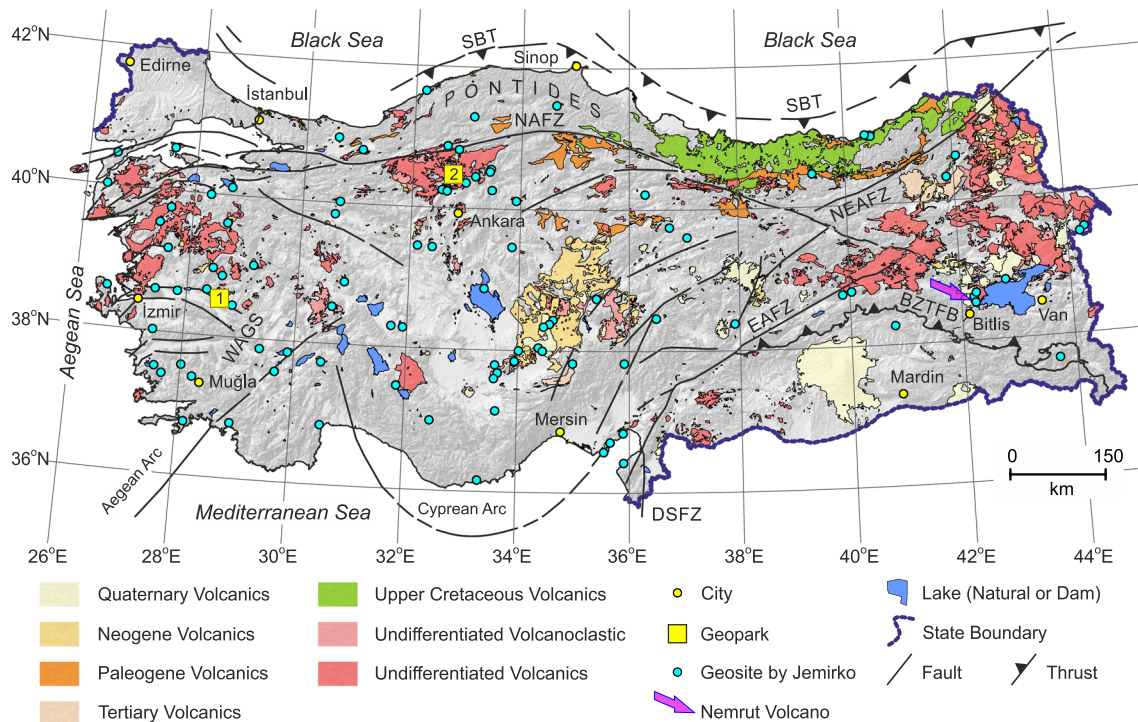


**Fig. 1** The global location of Anatolia (Turkey), geopark-geosite locations and volcanics across Anatolia (compiled from MTA (1964), Pawlewicz et al. (1997), Yiğitbaş et al. (2004), CGIAR-CSI GeoPortal (2012), Kazancı (2012), Akbulut (2014), Jemirko (2014, 2018)). The dashed lines on the figure show Turkish territory. Geosites by Jemirko marked on the map indicate discrete points or areas. Geoparks (the yellow squares) on the map show Kula (1 in this figure) and Kızılcahamam (2 in this figure) with their approximate locations, not their concrete areas.

Anatolia is a geographic terrain fragmented into tectonic elements. Abbreviations for the tectonic boundaries: BZTFB, Bitlis-Zagros Thrust and Fold Belt; DSFZ, Dead Sea Fault Zone; EAFZ, East Anatolian Fault Zone; NAFZ, North Anatolian Fault Zone; NEAFZ, Northeast Anatolian Fault Zone; SBT, Southern Black Sea Thrust; WAGS, West Anatolian Graben System. Faults and the thrust-fold belt on the map depict their traces, not accurate positions. The figure uses Lambert Conformal Conic projection with WGS 84 datum

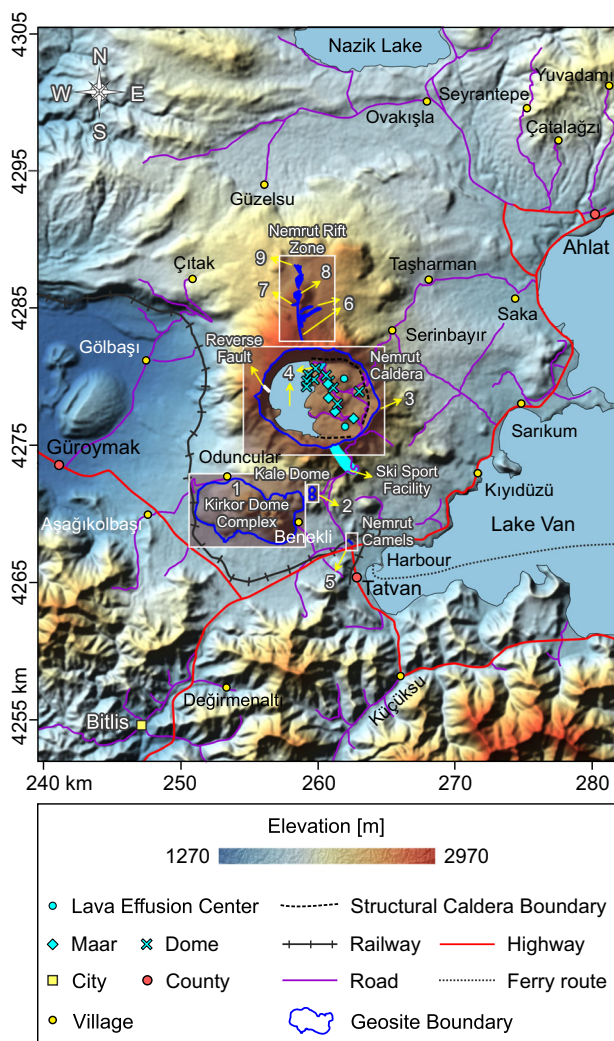


**Fig. 2** The spatial position of Nemrut Stratovolcano (Mt. Nemrut) and its adjacent terrain (compiled from NASA EarthData (2020); OpenStreetMap (2019); Ramsar (2019)). The structural caldera boundary is marked with black dashed lines. Blue-green coloured (cyan) dots at the caldera base designate the geomorphologic assets (maars, dome, and lava effusion centres). Blue lines and numbered areas indicate the geosites: 1 (Kirkor Dome Complex), 2 (Kale Dome), 3 (Nemrut Caldera); The geosite boundary overlaps with the site boundary of Ramsar (2019), natural monument boundary of MAF (2020), and almost Nemrut Caldera rim. The caldera includes the caldera wall (dikes, reverse faults, and structural caldera boundary; see details in Fig. 11) and the geomorphologic elements at the caldera base (domes, lava effusion centres, and maars; see details in Fig. 11), 4 (The cold lake or Nemrut Lake and hot lake with fumaroles and hot springs), 5 (Nemrut Camels), the rift zone: it includes 6 (The rift zone, the rift zone rhyolite or comendite rock, and 1441–1597 AD historical basaltic flows), 7 (1441–1597 AD historical basaltic-rhyolitic lava flows of the rift zone), 8 (1441–1597 AD rhyolitic lava lake of the rift zone), and 9 (1441–1597 AD historical rhyolitic and basaltic lava flows of the rift zone). The rectangular areas were added to indicate the position of the geosites more easily. The figure uses Universal Transverse Mercator projection with WGS 84 datum in 38 Northern Hemisphere Zone

sightseeing of natural sites) phase (Çetiner et al. 2018), with the exceptions of the Kızılcahamam (Kazancı 2012) and Kula (Akbulut 2014) geoparks (Fig. 1).

The first geopark experience models in Turkey are the Kızılcahamam (Kazancı 2012) and Kula Geoparks (Akbulut 2014). The Kula Geopark is also included in the European Geoparks Network (EGN). There are also local studies that have significantly focused on geotourism potential (Ateş and Ateş 2019; Gürer et al. 2019; Köroğlu and Kandemir 2019), geosite-geodiversity evaluations (Kazancı et al. 2007; Hatipoğlu 2010; Akbulut and Gülüm 2012; Güngör et al. 2012; Kopar and Çakır 2014; Kazancı and Gürbüz 2014; DAKA 2016; Çıtıroğlu et al. 2017; Üner et al. 2017; Uzun 2017; Erturaç et al. 2017; Kaygılı and Aksoy 2017; Kaygılı et al. 2017; Dölek and Şaroğlu 2017; Çetiner et al. 2018; Doğan et al. 2019), and geopark proposals (Akbulut 2011; Karahan et al. 2011; Gürler and Derman 2012; Gürler et al. 2013). The Turkish Association for the Protection of Geological Heritage (Jemirko in Turkish) catalogued geosites across Turkey based on personal suggestions (Fig. 1) (Jemirko 2014, 2018). Nemrut volcano and its periphery were also proposed as geosites in the Jemirko catalogue. In this unpublished catalogue, Nemrut caldera is a massive geosite. The Kantaşı (Nemrutbaşı) dome and Nemrut caves (Nemrut Kervanı) around the caldera periphery have been documented due to their geo-specific features (Jemirko 2014, 2018). Nemrut volcano was also reported to be a massive geosite by Dölek and Şaroğlu (2017). Üner et al. (2017) described the geoheritage value of earthquake-induced structures on the eastern coast of Lake Van. Nemrut volcano is catalogued and classified (Jemirko 2014, 2018) as a natural beauty site (for unique and complete sightseeing); additionally, the caldera has been considered a (geo)tourism spot without estimation procedures (Gürbüz 1995; Akbulut 2014; DAKA 2016; Kaygılı et al. 2018). Each of these publications has displayed primitive views about Nemrut volcano without any methodological scheme. The scope of this study is to present an inventory of site-specific (Fig. 2) geodiversity values for Nemrut caldera using the methodology of Brilha (2016) for geotourism-geopark development.

### Synopsis of Eastern Anatolian Tectonic Setting

Eastern Anatolia is a geographic region in the eastern part of Turkey with a mean elevation of ~2 km. The elevation reaches up to 5150 m (Fig. 3). The topographic relief is mainly the result of continent-continent collision and extensional regimes (relay zones) that are linked to Plio-Quaternary volcanoes (Koçyiğit et al. 2001; Dhont and Chorowicz 2006; Ulusoy 2008). The continent-continent collision was N–S directed, and post-collisional intracontinental convergence continued to the end of the Late Miocene and into Early Pliocene

(Koçyiğit et al. 2001). The uplift connected to the collision formed the high plateau (~2 km) that exists at present, so the region is also known as the Eastern Anatolia Plateau. The trace of the collision on the topography forms the Bitlis-Zagros Thrust Fold Belt (BZTFB in Fig. 1). The younger segments of the BZTFB are situated in the southern region (Emre et al. 2018). The southern segments of the thrust fold are active faults known as the South-East Anatolian Thrust Zone (SEATZ in Fig. 3). This zone is characterized by low-angle thrust faults and is more than 600 km in length (Emre et al. 2018); the thrust zone extends from Hakkari city on the Turkish border to the region south of Bingöl city (Fig. 3). An earthquake (M 6.6) produced a surface rupture on the SEATZ, with the epicentre located in the northernmost part of the SEATZ (Fig. 3).

The East Anatolian Fault Zone (EAFZ) is a strike-slip fault zone with a NE-SW direction. The portion of the fault from Karlıova County to Bingöl city is shown in Fig. 3. The strand to the southwest of the EAFZ cuts the SEATZ. The surface ruptures developed on the EAF occurred due to an earthquake (M 6.8) in Bingöl, as shown in Fig. 3. The North Anatolian Fault Zone (NAFZ) is a strike-slip fault system, the eastern branch of which extends from Karlıova. Karlıova is the conjunction point of the EAFZ and the NAFZ (Fig. 3) and is known as the Karlıova triple-junction point (Emre et al. 2018). A recorded earthquake (M 6.0) in the NW region of Karlıova along the eastern branch of the NAFZ is shown in Fig. 3 (Emre et al. 2013). The North-Eastern Anatolian Fault Zone (NEAFZ), a strike-slip fault zone, lies in the northernmost part of Eastern Anatolia and consists of several segments (Bozkurt 2001). The Eastern Anatolian segments of the NEAFZ elongates SW-to-NE south of Artvin (Fig. 3). No historical or recent seismic event has been recorded along the northern segment of the NEAFZ so far (Koçyiğit et al. 2001). The sinuously shaped fault traces extending from Erzurum-Ardahan are shown in Fig. 3. The segments are almost parallel. The flat topographic surfaces around Erzurum and Ardahan (Fig. 3) are pull-apart basins bounded by fold-shaped hills accompanying the sinuous fault traces (Dhont and Chorowicz 2006). Some segments bounding the Erzurum basin to the west and east are also active fault segments (Fig. 3). A curved fault in the north of Kars progressively changes from an E-W-trending to a NE-SW-trending strike-slip fault (Dhont and Chorowicz 2006). The SW end of the fault is an active fault component that produced an earthquake of M = 6.8 (Emre et al. 2013). Kars city and the nearby areas are bounded by a normal fault to the south. This terrain is known as the Kars Volcanic Plateau (Dhont and Chorowicz 2006). Several extensional fractures are deduced from the volcanoes that lie linearly along the SW-NE direction (Fig. 3). These extensional fractures and fissures are well exposed at the summits of Plio-Quaternary volcanoes (Koçyiğit et al. 2001). Prominent examples of volcanoes,

from north to south, include the Ağrı, Tendürek, Süphan and Nemrut volcanoes (Fig. 3). Tendürek and Nemrut are characterized by extensional fissures. The fissure situated on the northern side of Nemrut volcano is known as the Nemrut rift zone, as shown in Fig. 2, or the Nemrutbaşı dome (Kantaşı hill), shown in Fig. 4. The Muş Basin elongates on the western side of Nemrut volcano (Fig. 3); this basin is the deformed and dissected remnant basin of the Oligo-Miocene Muş Lake Basin (Koçyiğit et al. 2001). The Muş Basin is delimited to the north by a fault (Fig. 3) that is known as the Otluk fault (Otf) or Gedikpınar rise (Fig. 4). This active fault is considered a dextral oblique-slip fault (Dhont and Chorowicz 2006) or left-lateral reverse fault (Emre et al. 2013). Earthquake data have not been recorded along the Otluk fault or along the periphery of Nemrut caldera (Emre et al. 2013). Obviously, the locations of earthquake in Eastern Anatolia are distributed in a linear form with different magnitudes ( $M \geq 5.5$ ) along the active faults. These earthquakes result from seismogenic depths or crustal structures and from the different plate and lithospheric components of active tectonics around Turkey (Koçyiğit et al. 2001; Emre et al. 2013). The highest-magnitude earthquakes ( $M \geq 7.0$ ) in Eastern Anatolia (Fig. 3) were recorded during the surface rupture of the active fault (M 7.0) situated on the north-eastern side of Lake Van and during the surface rupture of the active fault (M 7.2) on the eastern side of Lake Van (Emre et al. 2013).

## Geology of Nemrut Volcano

Mt. Nemrut is a quiescent Quaternary volcano in Eastern Anatolia situated near the western shore of Lake Van. The eruption centre of the volcano is located near Bitlis city and Tatvan County (Fig. 2). The volcano has an elliptic summit caldera with a diameter of  $\sim 8.6 \times 7$  km. The caldera's apex is approximately 2900 m in elevation.

The volcano evolved on the pre-volcanic basement rocks. The basement rocks shown in Fig. 4 are composed of Bitlis metamorphic rocks in the south and Tertiary sediments in the north (Ulusoy et al. 2012). Other volcanic centres are located in the proximity of Nemrut volcano. The Kolango dome comprising Bilican volcano is located to the northwest of Nemrut volcano (Fig. 4). A NW-SE-inclined lineament crosses the peak of the dome, and a WNW-ESE-inclined rift passes through the dome towards (Ulusoy 2008). The pre-volcanic basement and Bilican Volcanics (Kolango Dome in the inventory site) are categorized into the basement rock section of the geologic map (Fig. 4). The volcanic products that formed on the pre-volcanic basement also classified into pre-caldera, syn-caldera (caldera-forming), and post-caldera phases, as described below.

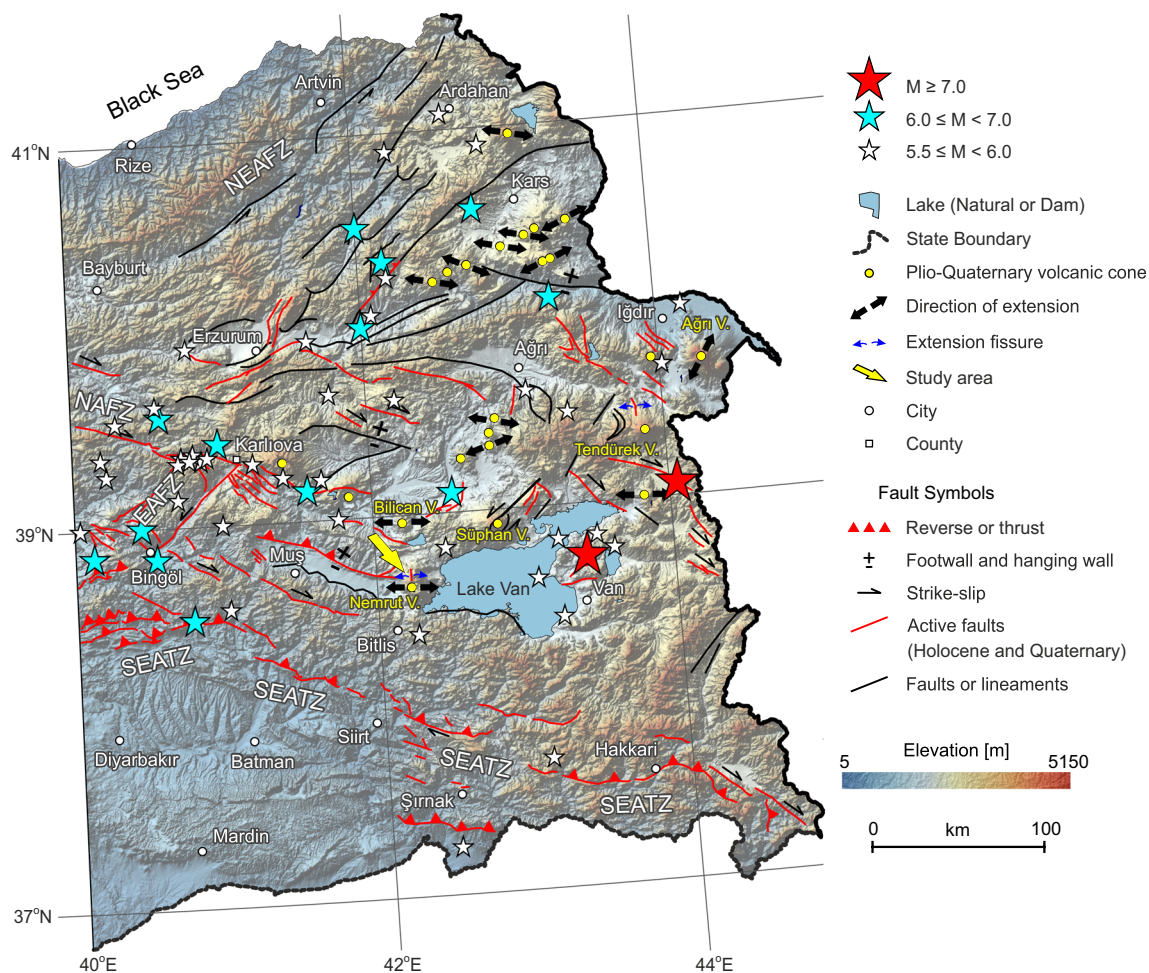


**Fig. 3** Tectonic setting map for Eastern Anatolia (compiled from Dhont and Chorowicz (2006); Emre et al. (2018)). The dashed lines show Turkish territory. Abbreviations of the tectonic elements: SEATZ, Southeast Anatolian Thrust Zone; EAFZ, East Anatolian Fault Zone;

NAFZ, North Anatolian Fault Zone; NEAFZ, Northeast Anatolian Fault Zone. The earthquake dataset on the map was obtained from (KOERI 2021). The figure uses Lambert Conformal Conic projection with WGS 84 datum

### Pre-caldera Stage of Nemrut Volcanism

The pre-caldera stage of Nemrut volcanism (volcanic activity) occurred between  $1.01 \pm 0.04$  Ma and  $80 \pm 20$  ka (Ulusoy et al. 2012). The inner phases of the pre-caldera stage consisted of edifices of the volcano represented by lava flows and peripheral doming centres with related lava flows (Ulusoy 2008; Çubukçu et al. 2012). The products related to the oldest (initial) phase, here meaning the oldest known lava flows at Nemrut (Stratigraphic ID (SID): 1080, as shown in Fig. 4), are represented by silica-oversaturated trachytes and comendites. The initiation of volcanic activity in the pre-caldera stage was dated by the K-Ar radiometric method on a rock sample taken from a trachyte outcropping on the western wall of the caldera (Ulusoy et al. 2012). The age of  $1.01 \pm 0.04$  Ma obtained from the trachyte sample is suspicious in terms of indicating the onset of volcanic activity, as this measurement was not observed at the base of the trachyte unit from the pre-caldera stage (Çubukçu 2008). The younger unit comendites on the

western wall of the caldera were dated as  $567 \pm 23$  ka. According to these ages, the oldest lava low activity began with trachytes at least and continued with comendites. During the pre-caldera stage, the younger and stratigraphically top-most volcanic succession displayed temporal evolution from a trachytic-with-pantelleritic-type and comenditic trachytes to comendite composition (SID: 1070 in Fig. 4). The sampling locations of the pantelleritic trachytes and comendites are south of Yumurtatepe village and northwest of Oduncular village, respectively. K-Ar dating of the samples yielded ages of  $384 \pm 23$  ka for the pantelleritic trachytes and  $310 \pm 100$  ka for the comendites (Çubukçu 2008).

The volcanic activity of Nemrut volcano continued to produce lava flows after  $\sim 300$  ka and produced marked trachytic and rhyolitic (comendite, comenditic trachyte) lavas (SID: 1060 in Fig. 4). Moreover, some exterior eruption centres (domes in Fig. 4) displaying ring shapes near the volcano were formed in this stage. The Kirkor dome complex (Gökgören Mountain) and the Yumurtadağ, Kalekırın, Kerkorumıksi,

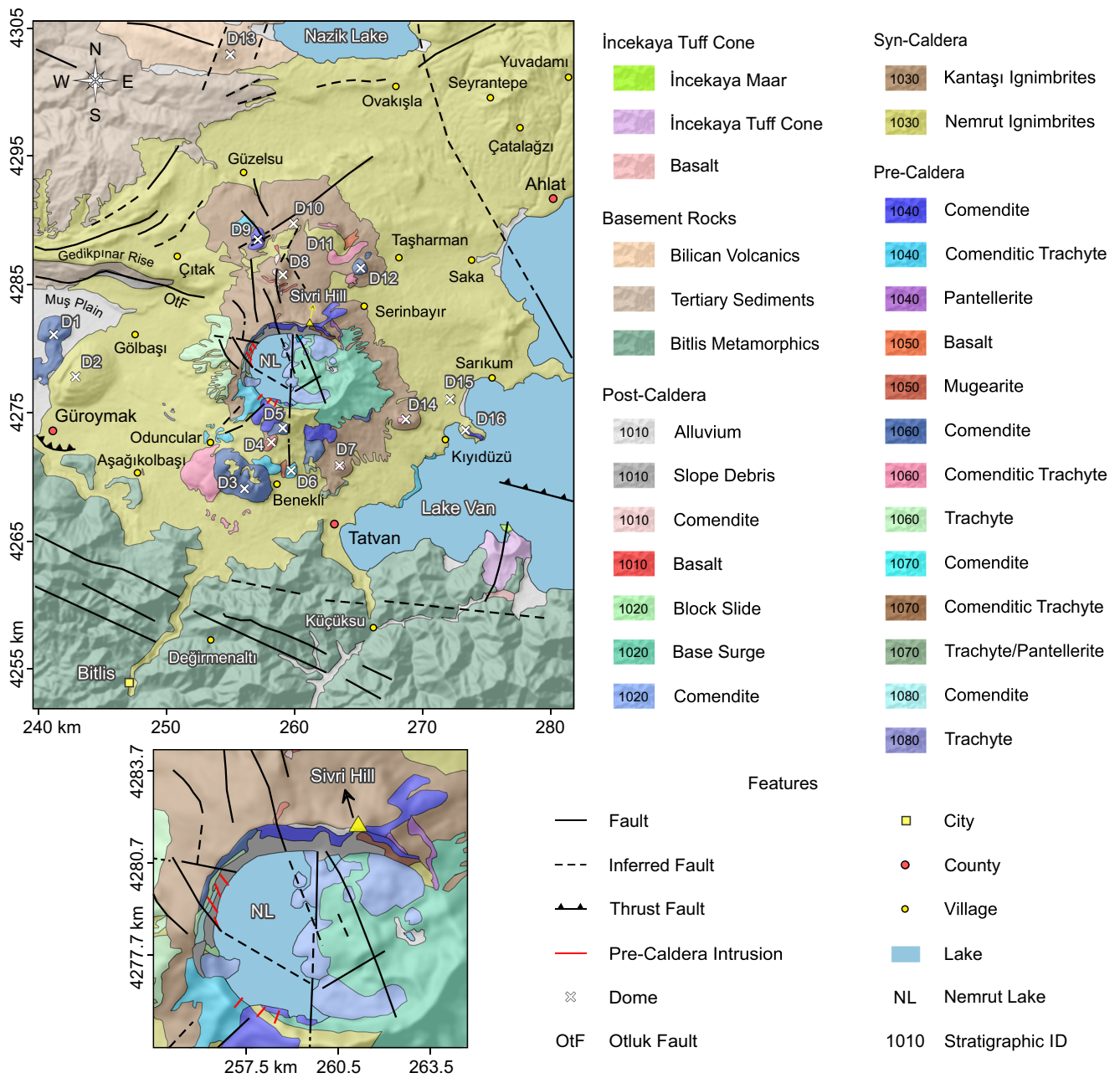


**Fig. 4** Geological map of Nemrut Stratovolcano and its adjacent terrain (compiled with Dhont and Chorowicz (2006); Çubukçu (2008); Ulusoy et al. (2008); Çubukçu et al. (2012)). The morphotectonic names for Otluk fault (OtF) and Gedikpınar rise are from Dhont and Chorowicz (2006) and Çubukçu (2008), respectively. The cross symbols refer to the domes: **D1** (Germav), **D2** (Mazik), **D3** (Kirkor dome complex), **D4** (Kerkorumiksi), **D5** (Kalekiran), **D6** (Kale), **D7** (Yumurtadağ), **D8** (Nemrutbaşı dome or Kantaşı hill), **D9** (Girigan), **D10** (Arizin), **D11**

(Tavşan), **D12** (Kayalı), **D13** (Kolango), **D14** (Fakı), **D15** (Yumurta), and **D16** (Meşeli or Meşelik). Pre-caldera intrusions (red lines) show dykes. Kirkor dome complex (**D3**), Kale dome (**D6**), the caldera (the closer view in the inset figure), Nemrut Lake (NL), and the nearby area of Kantaşı hill (**D8**) were evaluated as geosites (Fig. 2) of Nemrut Volcano and its adjacent terrain. The figure uses Universal Transverse Mercator projection with WGS 84 datum in 38 Northern Hemisphere Zone

and Kale domes are located south of the volcano. In contrast, the Nemrutbaşı dome (Kantaşı hill) and the Girigan, Arizin, Tavşan, and Kayalı domes occur on the north side of the volcano. The Kolango dome (Otluk Mountains), which is a separate volcano centre and is not considered part of Nemrut volcanism (Ulusoy 2008), lies far away from the northern

flank of Nemrut volcano. On the eastern flank of Nemrut volcano, the Fakı, Yumurta, and Meşeli (Meşelik) domes are situated. The Mazik and Germav (Girekol) domes bound the Muş Basin (Muş Plain) on the western side of Nemrut volcano (Fig. 4). The ring-shaped setting of the domes is interpreted as being due to the effect(s) of a circular or radial magma

chamber under a local E-W-extension stress regime (Ulusoy 2008). The presence of a shallow magma chamber is also supported by a recent geophysical study (Ekinci et al. 2020a). These domes are considered to belong to the pre-caldera stage, developing before the caldera-forming eruptions were linked to the stratigraphic setting, as the peripheral eruption centres, except for Germav (Girekol) dome, are either partly overlain by thick and extensive pyroclastic cover (Nemrut and Kantaşı ignimbrites in Fig. 4) or observed with remnant pyroclastics at their summits (Kirkor dome). In terms of radiometric data, the Kirkor dome complex and Kalekiran-Kerkorumıksi domes were dated at  $242 \pm 15$  ka and  $158 \pm 4$  ka, respectively (Çubukçu 2008). It is concluded that the beginning of peripheral doming, at least in the well-exposed southern area, could be limited to ages older than 160 ka (Çubukçu 2008).

Nemrut volcanism continued with basaltic and mugearitic lava flows (Çubukçu 2008). The mugearitic flows (SID: 1050 in Fig. 4) outcrop scarcely and are overlain by ignimbrites around Benekli village at the southern flank of the volcano, with a flow direction from Kale dome onto Kerkorumıksi dome, in the vicinity of Aşağıkolbaşı village and at the southern extremity of Nemrut rift; in other words, these flows are located to the south of Nemrutbaşı dome (Fig. 4). The basaltic outcrops are small and covered by ignimbrites (Ulusoy 2008), but a mapped outcrop can be observed around Taşharman village (Fig. 4). Mugearitic lava dated by Notsu et al. (1995) yielded a K-Ar age of  $100 \pm 50$  ka. The location from which the sample was obtained on the northwest caldera wall is unclear (NE-22 sample of Notsu et al. (1995)). Mugearite was most likely sampled from a point that was overlain by ignimbrites. It is also clear that the outcrops of mugearite lava shown in Fig. 4 are scarce and partially overlain by ignimbrites, so it is not possible to distinguish their lower boundary relations with relatively older rocks to deduce their stratigraphic setting. Provided that this is intended to be a broad statement, the structural relations and lower boundary contacts among the peripheral lava domes and lava flows cannot be gathered by field surveys to derive the sequence of volcanism (Çubukçu 2008).

The younger lava flows contain pantellerites, comenditic trachytes and comendites (SID: 1040 in Fig. 4). Pantellerite crops out only along the caldera rim at the upper elevations on the northeast flank of the volcano (Fig. 4). A pantellerite sample collected from this slope was dated to  $99 \pm 3$  ka (Çubukçu 2008). Comenditic trachytes are observed on the shoreline of Lake Van and on the flat land near Oduncular village. Each lava flow location in the coastal region of Lake Van was dated as  $93 \pm 3$  ka, and those near Oduncular village were dated as  $89 \pm 2$  ka (Çubukçu 2008). Above the elevation of the village, comenditic trachytes and comendites are in contact and lie along the south-eastern caldera rim (Fig. 4). Comendite lava protrudes from Sivri Hill (the northeast apex of the caldera rim

in Fig. 4) to Serinbayır village, near the north-western region of the rift zone to the north of the volcano, on the cape in close proximity to Kıyıldüzü village and on the southwestern flanks of the volcano in the recent topography (Fig. 4).

### Syn-caldera Stage of Nemrut Volcanism

Subsequent to the pre-caldera stage, the syn-caldera (caldera-forming) stage is the main stage in which the widespread pyroclastics named Nemrut and Kantaşı were produced. The pyroclastic eruption event ages are confined as approximately 90 ka by the youngest products dated before the caldera formation. Thus, younger ages are plausible for pyroclastic units between at least 89 ka and 30 ka (Çubukçu 2008). The pyroclastic sheets include felsic fallout tephra at the bases and overlying ignimbrite unit(s) at the tops (Çubukçu et al. 2012; Ulusoy et al. 2012). The Nemrut ignimbrites (Ulusoy et al. 2012; SID: 1030 in Fig. 4) are the most voluminous product and are observed above the Nemrut fallout units (Ulusoy et al. 2012). At the tops of the Nemrut ignimbrites, Kantaşı fallout units appear (Ulusoy et al. 2012). The pyroclastic sheet continues with Kantaşı ignimbrites (Ulusoy et al. 2012; SID: 1030 in Fig. 4). In Fig. 4, the Nemrut pyroclastics have the largest outflow sheet in the study site, and Nemrut ignimbrites are seen on the flatlands as well. Kantaşı ignimbrites are also observed dominantly to the north of the caldera. Each ignimbrite sheet is observed overlying the older lava flows, domes and even dikes that are exposed on the western and southwestern caldera walls. The dikes cut all units that outcrop on the caldera wall and are covered by ignimbrites (Fig. 4), so they formed in the pre-caldera stage (Ulusoy et al. 2012). Özdemir et al. (2006) assumed, on contrast, that the dikes belong to the post-caldera stage. If this assumption is credible, lava flows must have occurred before the caldera-forming stage instead of dikes (Çubukçu 2008).

### Post-caldera Stage of Nemrut Volcanism

Following the intense pyroclastic eruption, the post-caldera stage began. Activity from this stage is seen in the eastern part of the caldera and in the northern (Nemrut) rift zone (Fig. 4). The rift zone is remarkable, as the activity observed in this area represents the latest volcanic activity (1441, 1597, and 1692 (?) AD) described in the chronicles and manuscripts (Şerefhan 1597; Karakhanian et al. 2002; Aydar et al. 2003). Before rift development, phreatomagmatic/phreatic activity (the latest of which occurred in  $787 \pm 25$  and  $657 \pm 24$  BC) was dominant. The products of this activity include intra-caldera comendite lava flows/domes and phreatomagmatic (ash) deposits (SID: 1020 in Fig. 4). The intra-caldera comendite lava flows/domes yielded an age of  $15 \pm 1$  ka. The phreatomagmatic/phreatic products that partly cover the comendite lava and domes comprise comendite-base surge

and comendite lava. The base surge yielded an age of  $8 \pm 3$  ka and is more widespread than the comendite lava. The base surge overlies the ignimbrite succession on the eastern flanks of the volcano and can be seen in the caldera (Çubukçu et al. 2012; Ulusoy et al. 2012). The basalt and rhyolite (comendite) lava flow and lava fountains are the products of activities that occurred in 1441 (Karakhanian et al. 2002) and most likely before 1597 AD (Aydar et al. 2003; Ulusoy 2008). These rocks outcrop in the Nemrut rift zone formed (SID: 1010 in Fig. 4). However, the latest lava flow activity, indirectly noted by Şerefhan (1597) as a canal through which dark water (heavier than iron) flowed, was described to the north of the cold-water lake. According to the historical description, the latest volcanic activity continued to at least the year 1597. The imprecise locations of these activities indicate the rift zone in the northern part of the stratovolcano with reasonable confidence (Ulusoy et al. 2012). These locations are thought to be congruent with the analytical data referring to the younger ages measured inside the caldera ( $15 \pm 1$  ka and  $8 \pm 3$  ka) under the assumption that rift activity proceeded from south (the inner caldera) to north. The last historical activity of 1692 described in the chronicles (Karakhanian et al. 2002) formed no surface products (Ulusoy 2008; Ulusoy et al. 2012). Rift activity occurred between the Nemrut Plain and Kantaşı dome (hill) north of the caldera rim (Fig. 4). Kantaşı ignimbrites encircle the vicinity throughout the rift and the ridge (Kantaşı hill). The rifting cracked the ignimbrites, and basaltic/comenditic lavas flowed over the ignimbrites in east-west directions and welded on hilltops through the rift. The rifting is a result of the extensional regime (relay zones) in the Eastern Anatolia Plateau (Koçyiğit et al. 2001; Dhont and Chorowicz 2006; Ulusoy 2008).

### Structural Features of Nemrut Volcanism

Fissures or local extensional faults are exposed as discontinuities at the summits of volcanic edifices (Koçyiğit et al. 2001). The rifting is discontinuous, as the N-S-elongated extensional fault slightly bends in a NW-SE direction in the south (Fig. 4). The N-S directed structure with NNW-elongated faults inside the caldera (Fig. 4) depicts a fragmented view of the basal plateau and terminates at the Kale dome on the southern flank of Nemrut volcano (Ulusoy et al. 2008, 2012). Hot lakes and fumaroles are observed at the conjunction points of faults in the northern region of the caldera (Fig. 4), exposing recent volcanism (Ulusoy et al. 2008). The western side of the N-S extension zone is filled with a cold-water body (lake) (Fig. 4). In addition to linearly aligned faults, arc-shaped faults occur on the northwest slopes of the volcanic edifice (Fig. 4). The caldera at the eastern termination of the Muş Plain causes an arc-shaped fault trace on the western slope because the Otluk fault (OtF in Fig. 4) is a dextral oblique-slip fault (Dhont and Chorowicz 2006) or a left-lateral reverse fault (Emre et al.

2013), and the radial emplacement of dikes (pre-caldera intrusions in Fig. 4) acted as shear forces on the fault (Ulusoy 2008). North of the Otluk fault (OtF), on the Gedikpınar rise shown in Fig. 4, the faults elongate in arc-shaped tracks resulting from the local extensional regime related to Plio-Quaternary volcanoes; notably, the Nemrut Stratovolcano and the Bilican volcano are located far north of the studied site. Because of the deformational regime and eruptive events, transported materials have accumulated in front of the Otluk fault and travelled down intra-caldera inclines (slope debris in Fig. 4). Transported materials fill the valleys, shores, and Muş Basin (alluvium deposits in Fig. 4).

The onset of Nemrut volcanism formed trachytic lavas (Ulusoy et al. 2019). The development of the central cone was associated with peralkaline rocks (comendites and pantellerites) and comenditic trachytes (Çubukçu 2008). Furthermore, the pre-caldera stage was characterized by peripheral silicic doming. The explosive eruptions produced pyroclastic fall/flow deposits known as Nemrut and Kantaşı ignimbrites (Ulusoy 2008; Ulusoy et al. 2012) during the syn-caldera stage. A sketch diagram (Fig. 5) shows pyroclastic fall/flow eruptions and pyroclastic flows in the caldera-forming (syn-caldera) stage. The post-caldera stage produced peralkaline-type rocks (comendite), younger phreatomagmatic eruptions (ash), and rift activities (Ulusoy et al. 2019). The phreatomagmatic eruptions (ash) are sketched in Fig. 5. Linear and arc-shaped faults related to volcanism intersect at the summit and on the slopes of Nemrut volcano (Ulusoy et al. 2008, 2012). The recent morphology of the caldera is also given in Fig. 5. Every event in the geologic processes that acted on or was formed by Nemrut volcano produced diverse abiotic lithologic elements as well as hydro-geomorphologic elements. This volcanic geodiversity was scored based on the site-specific conditions of the suggested geosites according to a given methodology in the following section.

### Methodology

The main requirements for assessing geosites are published information and data obtained by geologists who conducted geological mapping or research (Çetiner et al. 2018). One type of crucial required data is published geological maps containing geographical attributes that portray the complexity of landscapes. By using the relevant data, the abiotic elements of the natural environment can be classified into certain groups according to the selected methodology (Zwoliński et al. 2018). By doing so, the criteria applied in a given methodology not only permit comparisons among geosites (Çetiner et al. 2018) but also contrast with the background abiotic characteristics of natural environments with exceptional geodiversity values. These values range from obvious values,

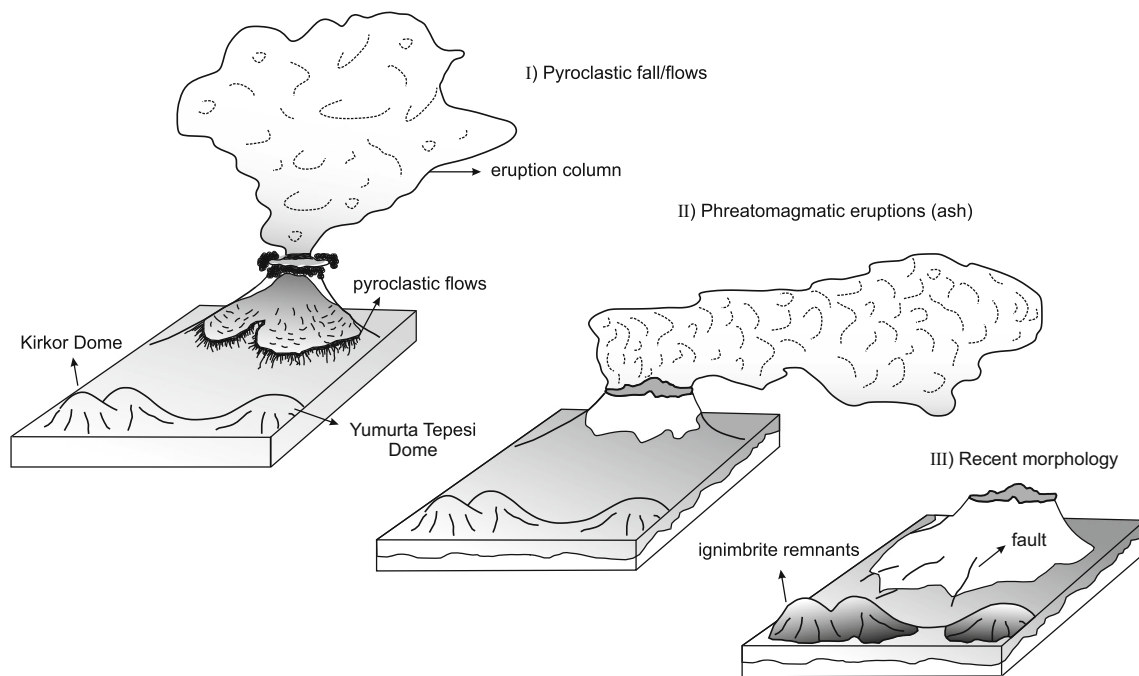


**Fig. 5** Sketch diagram of pyroclastic fall/flow eruption and pyroclastic flows in caldera-forming stage (syn-caldera stage) (modified after Karaoğlu et al. (2005))

such as economic (exploitation), scientific (working geosphere and interactions with Earth systems), and educational (geoscience teaching) values, to more intangible values, such as cultural and aesthetic values that can be applied in geotourism (Brilha 2018).

Regarding the short introduction provided herein, a linkage exists between the terms geosite and geodiversity. A geosite is a discrete point or concrete area defined by in situ geodiversity-related elements exposed on the Earth’s surface with high scientific, educational, aesthetic, and cultural values (Serrano and Ruiz-Flaño 2007; Ruban 2010; Brilha 2018). Several terms are associated with geodiversity, including geomorphosites (Rypl et al. 2016), geotopes (Serrano and Ruiz-Flaño 2007), geoparks (EGN 2020), geoconservation (Gray 2013), geoheritage (Dingwall et al. 2005), and geodiversity sites (Brilha 2016). These terms encompass different scales at supranational, national, and subnational levels. Geodiversity is inclined to jargon inflation. The term geosite is used here to encompass all scales used in any inventory scheme, from the simplest scheme comprising a few geosites to complex geosite inventories for scientific and touristic relevance, and so on (Çetiner et al. 2018).

The literature contains numerous examples of inventories (Brilha 2018) and assessments (Zwoliński et al. 2018). Geodiversity inventory or assessment techniques comprise any function or several functions, including classifications-descriptions of geodiversity attributes, valuations of attributes from utilitarian-scientific perspectives, weightings-numerations of attributes for comparisons, and the creation of attribute maps to examine their spatial distributions. First,

the method chosen for a geodiversity evaluation is based on expert or intuitive knowledge, as defined by Zwoliński et al. (2018). Without this step, the management of in situ geoconservation (geopark) in a territory is not complete (de Lima et al. 2010). This step is necessary for countries such as Turkey to such a degree that it has not completely advanced from the conservation phase thus far (Çetiner et al. 2018), with the exception of the Kızılcıhamam (Kazancı 2012) and Kula (Akbulut 2014) geoparks. The regional geosite catalogue of Turkey compiled by Jemirko (2014) reflects descriptive content based on verbal expert knowledge and supports the above statement (Çetiner et al. 2018) regarding the status of Turkey based on the definition given by Zwoliński et al. (2018). Further support for the statement comes from Çetiner et al. (2018) in the form of a scientific project related to the selection of geosites in the national parks of Turkey (Kazancı et al. 2007) and the need for verbal-descriptive information about the standardization of geodiversity-related assets in Turkey (Nizamettin et al. 2015; Çiftçi and Güngör 2016). Hereby, the conservation phase is still active. A national geosite inventory is in the embryonic stage in Turkey. In brief, a solid inventory method should not be scale dependent. That is, it should allow comparisons among geosites and intend to define the topic and use of a site within set criteria such as *scientific value* and *potential touristic use*. Here, the method suggested by Brilha (2016) was used to build a compact inventory scheme that suits the necessities and scores the criteria based on a user’s perception (semi-quantitative assessment).

## Semi-quantitative Assessment of Scientific Value

Brilha (2016) states that geosite selection according to *scientific value* (SV) should designate certain geological object(s) or process(es) in a study area in which related scientific data have been obtained and published. Each potential geosite must be qualitatively evaluated based on the criteria proposed according to *representativeness, integrity, rarity, and scientific knowledge*. The evaluation of geosites is vulnerable to subjectivity. For a quantitative assessment of *scientific value*, the method of Brilha (2016) was proposed to, at the very least, lessen the subjectivity of the *scientific value* criterion. In this method, each geosite is given a score of 1, 2, or 4, per the indicators for each criterion (Table 1). An indicator can also be zero when necessary but cannot obtain a score of 3 to ensure contrast with geosites having the highest score of 4 (Brilha 2016). The total geosite *scientific value* score for each geosite is a weighted sum of the seven criteria given in Table 2. Based on our understanding, a higher *scientific value* score mostly involves greater geosite values from the utilitarian perspective when a scientific base is established and many types of geodiversity are observed. This perception involves managing the assets of geosites by means of geopark and geotourism development with associated facilities to improve visitor experiences.

## Semi-quantitative Assessment of Potential Touristic Use

*Potential touristic use* (PTU) includes the following criteria defined by Brilha (2016): *vulnerability, accessibility, limitations, safety, logistics, population density, association with other values, scenery, uniqueness, observation conditions, interpretative potential, economic level, and proximity of recreational areas*. The scores vary from 1 to 4, including scores of zero for the assessment of the criteria (Tables 3 and 4). The final evaluation of the touristic value of each geosite is given as the total geosite *potential touristic use score*, which equals the weighted sum of all scores (Table 5). The higher the *potential touristic use* value a given geosite is, the higher the proportion of visitors that would be satisfied if an intrinsic element of the geosite is easily seen. In some cases, a higher *potential touristic use* value can indicate preferable ex situ geosite conditions, such as *accessibility, safety, logistics, and economic level*. A good combination of conditions is much more affordable for geopark and geotourism services. One assessment method considers the *potential touristic use* and *scientific value* scores and includes ex situ and in situ geosite conditions. Thus, the method allows decisions to be made regarding the balance of scientific and management outcomes (utilitarian-scientific perspective) for each geosite.

## Description of Nemrut Volcano Geosites

The geosites shown in Fig. 2 are grouped into the domes (geosites 1 and 2), the caldera, including the caldera wall and the caldera base (geosite 3), the lakes, including hot and cold lakes (geosite 4), the Nemrut camels (fairy chimney formation) (geosite 5), and the rift zone (geosites 6, 7, 8, and 9).

The largest outflow sheet across the study site contains Nemrut and Kantaşı ignimbrites on which the Nemrut camels formed (Fig. 4). The ignimbrites formed shallowly sloping flanks and flatlands adjacent to the caldera. The slope map (%) given in Fig. 6a shows the entire study area and the geosite boundaries. Land surfaces with slopes less than 30% cover a large area in this region. According to our interpretation, a terrain slope greater than or equal to 30% can result from a fault scarp (Gedikpınar rise in Fig. 6a), collapse structure (the caldera wall) or slump structure. Slump structures are found on the northern and eastern shallowly sloping flanks of the volcano and on the ignimbrite sheet (Fig. 6a). Nemrut ignimbrites are also characterised by flatland landforms. The morphologic map of Nemrut volcano shows a heterogenic distribution and patterns of ridges and valleys (Fig. 6b). The valleys and ridges on the eastern shallowly sloping flanks are longer than the valleys and ridges on the western flanks. A different pattern is observed on the northern and eastern low-slope flanks of the volcano. The ridges are long, but the density is lower on the northern flanks than on the eastern and western flanks of the volcano. According to our interpretation, the northern flank is characterised by diffused pyroclastic flows of Nemrut and Kantaşı ignimbrites and plateau landscapes (Fig. 6a). The caldera and rift zone display steep topography (Fig. 6a), stimulating aesthetic perceptions, so these areas are considered highly unusual geosites. This steep topography reveals higher geological diversity rather than plateau morphology and shallowly sloping landforms. Although steep topography is thought to trigger natural hazard occurrences (e.g., landslides, rockfalls, avalanches, and floods), Fig. 7 shows that these events do not occur around Nemrut volcano. The data reveal that the natural hazard occurrences are centred on the basement rocks shown in Fig. 4. The earthquake locations ( $M \geq 5.5$ ) are distributed in a linear form along the active faults that are related to plate and lithospheric components in Turkey (Koçyiğit et al. 2001; Emre et al. 2013). Therefore, the volcano and its close vicinity are the most suitable areas for inventorying and assessing geosites.

The Kirkor and Kale domes of the pre-caldera stage are geomorphological (geomorphosite) geosite types. The caldera formed in the syn-caldera stage is a massive geosite consisting of the amalgamation of structural (caldera wall) and geomorphologic (maars domes and effusion centres at the caldera base) elements. The Nemrut camels, a syn-caldera product, outcrop in a dissimilar geomorphosite oriented in the NW direction near Tatvan County. This site is known as the

**Table 1** Criteria, indicators, and parameters for the scientific value of geosites (Brilha 2016)

Criteria/indicators of scientific value (SV)	Parameters (points)
<b>Representativeness<sup>a</sup></b>	
The geosite is the best instance representing features or processes in the study site	4
The geosite is a good instance representing features or processes in the study site	2
The geosite represents features or processes plausibly in the study site	1
<b>Key locality<sup>b</sup></b>	
The geosite is admitted to GSSP or ASSP by the IUGS or is an IMA reference site	4
Utilization of the geosite by the international science community	2
Utilization of the geosite by the national science community	1
<b>Scientific knowledge<sup>c</sup></b>	
Publications about the geosite in international scientific journals	4
Papers about the geosite in national scientific publications	2
Abstracts about the geosite in international scientific events	1
<b>Integrity<sup>d</sup></b>	
Very well preserved main geological features	4
The main geological elements are preserved but the geosite is not so well preserved	2
The main geological elements are quite altered with preservation problems in the geosite	1
<b>Geological diversity<sup>e</sup></b>	
Geosite consists of more than three types of discrete geological assets with scientific relevance	4
Geosite consists of three types of discrete geological assets with scientific relevance	2
Geosite consists of two types of discrete geological assets with scientific relevance	1
<b>Rarity<sup>f</sup></b>	
The geosite is the single type in the study site	4
The number of similar geosites in the study site is 2 to 3	2
The number of similar geosites in the study site is 4 to 5	1
<b>Limitations<sup>g</sup></b>	
Sampling or fieldwork do not depend on limitations	4
Collecting samples and fieldwork are available after overcoming limitations	2
Sampling and fieldwork are difficult owing to limitations that are difficult to overcome	1

GSSP, Global Boundary Stratotype Section and Point; ASSP, Auxiliary Stratotype Section and Point; IUGS, International Union of Geological Sciences; IMA, International Mineralogical Association

<sup>a</sup> Representativeness: the relevancy of the geosite to represent a geological process or feature

<sup>b</sup> Key locality: significance of a geosite as a reference for stratigraphy, mineralogy, etc.

<sup>c</sup> Scientific knowledge: scientific studies focusing on the geosite assets

<sup>d</sup> Integrity: connected to the conservation status of the main geological elements

<sup>e</sup> Geological diversity: amount of discrete geological elements related to scientific interest

<sup>f</sup> Rarity: amount of same type geosites in the study area

<sup>g</sup> Limitations: the state of obstacles (legal permissions, physical barriers, etc.) limiting for the regular scientific use of the geosite

Nemrut camels in the local community folklore. The hot and cold lakes are hydrologic geosites located in the inner caldera and indicate recent volcanism. The rift zone is also an indicator of the latest volcanism. The rift zone includes unique geosites with lithologic elements that include basalt and rhyolite flows with enclaves (lithologic elements) related to the historical events of 1441–1597 AD. The N-S-elongated rift zone can be viewed very clearly in the vicinity of Kantaşı Hill (Nemrutbaşı Dome), which is a part of the rift zone (Dome 8 in Fig. 4) and is described as geosite 8 herein (Fig. 2).

### Scientific Value Assessment of Nemrut Volcano Geosites

Table 6 shows the results of the *scientific value* assessment of the geosites of Nemrut volcano, including the indicators and the total geosite *scientific value* scores. The scores are also shown in Fig. 8. Snapshot views of the geosites are illustrated in Fig. 9, and the directions of the views are given in the Supplementary Information. The terms related to criteria and indicators are also

**Table 2** Criteria and their weights to assess the scientific value of geosites (Brilha 2016)

Scientific value (SV) criteria	Weight (%)
Representativeness	30
Key locality	20
Scientific knowledge	5
Integrity	15
Geological diversity	5
Rarity	15
Use limitations	10
Total geosite SV score	100

highlighted in italics to allow readers to understand the terms easily.

### The Domes

The Kirkor dome complex (Gökgören Mountain) and Kale domes (hills) are significant to assess first-hand among the ring-shaped domes (Fig. 4). The Kirkor dome has been dated (at  $242 \pm 15$  ka in Çubukçu 2008) and is peculiar, with remnant ignimbrites at its apex compared to other domes covered with pyroclastic products (Fig. 10a–c). The Kale domes are located at the end of the N-S-directed elongation (inferred fault) striking in the NW-SE direction to the south (Figs. 4 and 10d). Thus, these geosites (geosites 1 and 2) are the best examples depicting the pre-caldera stage before the syn-caldera stage of the pyroclastic succession (Kirkor dome) and the south termination of the inner caldera faults (Kale domes), according to the *representativeness* criterion (these sites were given scores of 4). The *key locality* of these sites can be used for reference models of peripheral doming structures at the national level (given a score of 1), but the same is not true for the rifting of the extensional regime due to the presence of localities representing better examples at the northern end of the rift zone. International scientific papers in which the domes were studied are available to analyse the use of these domes as geotourism sites on a conceptual basis (Kaygılı et al. 2018) and to study volcanic evolution (Çubukçu 2008; Ulusoy 2008; Çubukçu et al. 2012; Ulusoy et al. 2012) for the *scientific knowledge* criterion (given a score of 4). Related to *integrity*, each geosite is well preserved due to their locations in rural areas (given a score of 4). Kirkor and Kale domes are geomorphosites that each include one type of geodiversity asset: the doming structure representing the pre-caldera period and the south termination of the inner-caldera fragmented faults (the possible onset of rifting), as shown in Fig. 2 (given a score of 0 for *geological diversity*). Regarding the *rarity* of these sites, the Kirkor dome complex is not exceptional despite being the largest in size (given a score of 1), whereas the Kale domes are the only occurrence

coinciding with fault elongations (given a score of 4). The geosites have no *limitations* for sampling or fieldwork (given a score of 4). The indicator and total geosite *scientific value* scores of the domes are tabulated in Table 6 and shown on graphs in Fig. 8.

### The Caldera and the Lakes

The caldera (shown in a map view in Figs. 2 and 11a) formed in the syn-caldera stage is a massive geosite consisting of an amalgamation of geomorphologic features at the caldera base (domes, lava effusion centres, and maars, as shown in Fig. 11a) and structural features on the caldera walls (dikes, reverse faults, and the caldera boundary, as shown in Fig. 11a and b). The lakes are a hydrologic geosite (Fig. 11c). A panoramic view of the geosites (geosites 3 and 4) is shown in Fig. 11d. The syn-caldera (caldera-forming) stage is also the main stage in which widespread Nemrut and Kantaşı pyroclastics were produced, forming the shallowly sloping flanks of the volcano and the plateau landscape (Figs. 4 and 6a). However, *scientific value* features are mostly observed at the caldera base and the caldera wall as a result of the conjunction of eruptive/effusive volcanic rock outcrops and structural phenomena linked to fissures or local extensional faults (reverse faults). This steep topography reveals a higher geological diversity (criteria in Table 1) rather than a plateau morphology. Therefore, the caldera consists of the best examples depicting the syn-caldera stage, according to the *representative* criteria in Table 1. Certain types of geodiversity elements (geomorphologic and hydrologic elements) only occur within the depression zone (the caldera base) of the volcano and on the caldera walls. The wall between the topographic rim and the structural caldera boundary (Fig. 11a and d) has a unique feature among the geosites; fault displacement is visible at this location.

The geosites used to depict the syn-caldera stage were given a score of 4 as the best examples for *representativeness*. The *key locality* criterion for the sites can be applied at the international level (given a score of 2) because the caldera has both geopark and geoheritage (supranational) value due to its geodiversity in addition to its biodiversity and cultural (mythological and auxiliary) values. The argument we develop in this paper is given in the main section below (*Geopark Value of Nemrut Volcano*). Scientific documents related to the caldera and the lakes, such as documents describing their natural heritage (Özsoy 2010), the creation of a geotourism spot on a conceptual basis (Akbulut 2014; Kaygılı et al. 2018), and evolution in the geologic past (Çubukçu 2008; Ulusoy 2008; Çubukçu et al. 2012; and Ulusoy et al. 2012), are available, so *scientific knowledge* was scored at 4. In terms of *integrity*, each geosite is well preserved due to being part of a Ramsar site (Ramsar 2019) and a natural park designated by the Ministry of Agriculture and Forestry (MAF 2020). Hence,

**Table 3** Criteria, indicators, and parameters for the potential touristic use of geosites (Brilha 2016)

Criteria/indicators of potential touristic use (PTU)	Parameters (points)
<b>Vulnerability<sup>a</sup></b>	
No trace of potential deterioration of main geodiversity attributes by human activity	4
Prone to deterioration of secondary geodiversity attributes by human activity	3
Prone to deterioration of main geodiversity attributes by human activity	2
Prone to deterioration of the entire geodiversity attributes by human activity	1
<b>Accessibility<sup>b</sup></b>	
The distance of the geosite is 100 m or less from a paved road and with parking site	4
The distance of the geosite is 500 m or less from a paved road	3
Transferring to the geosite by bus on a gravel road	2
Geosite without direct access but less than 1 km away from a road	1
<b>Limitations<sup>c</sup></b>	
No limitations for utilization by students and tourists	4
The geosite can be utilized only time to time by students and tourists	3
The geosite can be utilized by students and tourists after overcome limitations (legal permissions, etc.)	2
Utilization is very difficult for students and tourists because of limitations to overcome (legal permissions, etc.)	1
<b>Safety<sup>d</sup></b>	
Less than 5 km from emergency services to the geosite with safety regulations and mobile phone coverage	4
Less than 25 km from emergency services to the geosite with safety regulations and mobile phone coverage	3
Less than 50 km from emergency services to the geosite without safety regulations and with mobile phone coverage	2
More than 50 km from emergency services to the geosite without safety regulations and mobile phone coverage	1
<b>Logistic<sup>e</sup></b>	
Distance of less than 15 km from the geosite to accommodations and restaurants for groups of 50 persons	4
Distance of less than 50 km from the geosite to accommodations and restaurants for groups of 50 persons	3
Distance of less than 100 km from the geosite to accommodations and restaurants for groups of 50 persons	2
Distance of less than 50 km from the geosite to accommodations and restaurants for groups of less than 25 persons	1
<b>Density of population<sup>f</sup></b>	
Geosite situated in a district where the population density is more than 1000 inhabitants/km <sup>2</sup>	4
Geosite situated in a district where the population density is 250–1000 inhabitants/km <sup>2</sup>	3
Geosite situated in a district where the population density is 100–250 inhabitants/km <sup>2</sup>	2
Geosite situated in a district where the population density is less than 100 inhabitants/km <sup>2</sup>	1
<b>Association with other values<sup>g</sup></b>	
Less than 5 km from the geosite to numerous ecological and cultural values	4
Less than 10 km from the geosite to numerous ecological and cultural values	3
Less than 10 km from the geosite to one ecological and one cultural value	2
Less than 10 km from the geosite to one ecological or cultural value	1
<b>Scenery<sup>h</sup></b>	
Current utilization of geosite as a tourism destination in national scale	4
Irregular utilization of geosite as a tourism destination in national scale	3
Current utilization of geosite as a tourism destination in local scale	2
Irregular utilization of geosite as a tourism destination in local scale	1

<sup>a</sup> Vulnerability: deterioration of geodiversity elements by visitors

<sup>b</sup> Accessibility: access to the geosite with transportation

<sup>c</sup> Limitations: obstructions for the progress of touristic events

<sup>d</sup> Safety: risk conditions for visitors

<sup>e</sup> Logistics: access to services such as accommodation and food for visitors

<sup>f</sup> Density of population: potential source of visitors for geosites

<sup>g</sup> Association with other values: the event of natural or cultural assets

<sup>h</sup> Scenery: aesthetic value of geodiversity features

**Table 4** Criteria, indicators, and parameters for the potential touristic use of geosites (Brilha 2016)

Criteria/indicators of potential touristic use (PTU)	Parameters (points)
<b>Uniqueness<sup>a</sup></b>	
Unique and rare assets taking into account the country and its neighbours	4
Unique and rare assets in the country	3
Common assets in the region interested but uncommon in different regions of the country	2
Rather common in the whole country	1
<b>Observation conditions<sup>b</sup></b>	
All geological features are observed clearly	4
Obstacles that result in difficulty with observation of some geological features	3
Obstacles that result in difficulty with observation of the main geological features	2
Obstacles that more or less obstruct the observation of the main geological features	1
<b>Interpretative potential<sup>c</sup></b>	
Geological features can be seen without difficulty and are demonstrative to laypeople	4
Layperson needs some background in geology	3
Layperson needs solid geological background	2
Expert level of geology required for understanding	1
<b>Economic level<sup>d</sup></b>	
The geosite is situated in a district where household income is at least the double of the national average	4
The geosite is situated in a district where household income is higher than the national average	3
The geosite is situated in a district where household income is equal to the national average	2
The geosite is situated in a district where household income is lower than the national average	1
<b>Proximity of recreational areas<sup>e</sup></b>	
The distance between the geosite and a tourist attraction is less than 5 km	4
The distance between the geosite and a tourist attraction is less than 10 km	3
The distance between the geosite and a tourist attraction is less than 15 km	2
The distance between the geosite and a tourist attraction is less than 20 km	1

<sup>a</sup> Uniqueness: the rarity of the geodiversity features to stimulate perception of visitors

<sup>b</sup> Observation conditions: clear observation of geodiversity elements from a layperson's view

<sup>c</sup> Interpretation potential: understanding capacity of geodiversity elements from a layperson's view

<sup>d</sup> Economic Level: the income level of people living close to the geosites linked to visiting prospects

<sup>e</sup> Proximity of recreational areas: earnings from the existence of touristic attractions in nearby area(s)

the geosites obtained scores of 4. The caldera is formed by the amalgamation of structural and geomorphologic elements consisting of more than three types of discrete geological assets with scientific relevance (given a score of 4). The lakes are hydrologic geosites illustrating recent volcanism (Ulusoy et al. 2008), so this geosite was scored at 0 for *geological diversity*. Regarding the *rarity* of these sites, Nemrut caldera and the lakes are unique among the geosites (given a score of 4). The geosites have no *limitations* for sampling or fieldwork (given a score of 4). The indicator and total *scientific value* scores for these geosites are given in Table 6 and placed on the graphs given in Fig. 8.

### Nemrut Camels

Nemrut ignimbrites formed the shallowly sloping flanks and flat terrain that are adjacent to the caldera. The erosional

realms of Nemrut ignimbrites (geosite 5 in Figs. 2 and 12a), which are syn-caldera products, outcrop in a unique geomorphosite (fairy chimney type) located to the NW of Tatvan County. The geosite or geomorphosite is known as the Nemrut camels, according to local community folklore. The geosite is unique. Consequently, it was given a score of 4 for the *representativeness* criterion. For the *key locality* criterion, the site has no significant value because no detailed studies related to the geosite have been conducted (Frödin 1937) or the existing studies are based on myths (folk tales) and popular science (Karaoğlu and Kılıç 2017). Folklore was recorded by Şerefhan (1597) regarding the mythological description known by the local community. In the Turkish translation from his Arabic manuscript, Nemrut volcano is called "Mount Nemruz," named after King Nemruz, who was believed to have lived there. The local community also believed that Nemruz (the King) spent winter around the mountain but

**Table 5** Criteria and their weights to assess the potential touristic use of geosites (Brilha 2016)

Potential touristic use (PTU) criteria	Weight (%)
Vulnerability	10
Accessibility	10
Limitations	5
Safety	10
Logistic	5
Density of population	5
Association with other values	5
Scenery	15
Uniqueness	10
Observation conditions	5
Interpretative potential	10
Economic level	5
Proximity of recreational areas	5
Total geosite PTU score	100

lived on the mountain in summer. King Nemruz, who was getting stronger day by day, destroyed all his enemies and

finally declared war on God (Karaoğlu and Kılıç 2017). The god let the mountain collapse as a result of wrath against the King, the lakes formed in the sink (the caldera) and a cloud of smoke covered all sides of the mountain. At the top of Nemrut volcano, the fire of King Nemruz appeared after the cloud of smoke disappeared, and the camel (Nemrut camels) caravans carrying wood to the fire of King Nemruz turned to stone (Karaoğlu and Kılıç 2017). The lack of interest in the Nemrut camels has led to their deterioration. The vulnerability of the rocks to erosion and urbanization (Fig. 12a, b) has attracted lessened attention in a popular sense (AA 2015). Although news stories have indicated that the Nemrut camels were authorized as a first-degree protected site, the protected asset(s) of the site was uncertain in the news (AA 2015). The historical (folkloric) value of this site was specifically indicated in a report (AA 2015) based on the Conservation Code of Natural and Cultural Properties (Legislation No. 2863) in Turkish Legislation Information System (Mevzuat Bilgi Sistemi or MBS in Turkish) (MBS 2020). A query conducted through the Protected Areas Management Information System (Sit Alanları Yönetim Bilgi Sistemi in Turkish) confirmed that the geomorphosite is registered as a historical-cultural site,

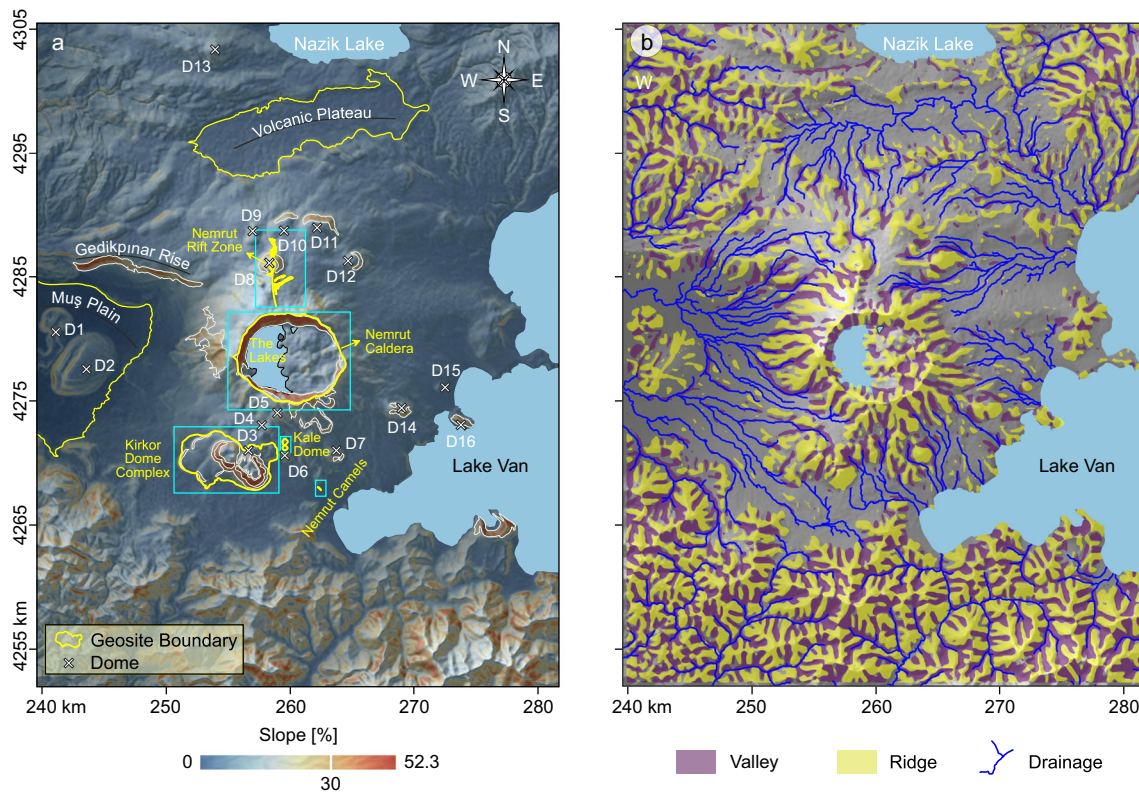


**Fig. 6** Slope (%) and morphometric map of Nemrut Volcano and nearby area; **a** the slope (%) map of Nemrut Volcano. The rectangular areas were added to indicate the position of the geosites more easily. Yellow lines on the map show geosite boundaries. The cross symbols refer to the domes: **D1** (Germav), **D2** (Mazik), **D3** (Kirkor dome complex), **D4** (Kerkorumıksi), **D5** (Kalekırın), **D6** (Kale), **D7** (Yumurtadağ), **D8** (Nemrutbaşı dome or Kantaşı hill), **D9** (Girigan), **D10** (Arizin), **D11**

(Tavşan), **D12** (Kayalı), **D13** (Kolango), **D14** (Faki), **D15** (Yumurta), and **D16** (Meşeli or Meşelik); **b** Morphometric map of Nemrut Volcano. Digital elevation model in the figure (DEM) were obtained from NASA EarthData (2020) and processed for morphometric features SAGA GIS (2020). The figure uses Universal Transverse Mercator projection with WGS 84 datum in 38 Northern Hemisphere Zone

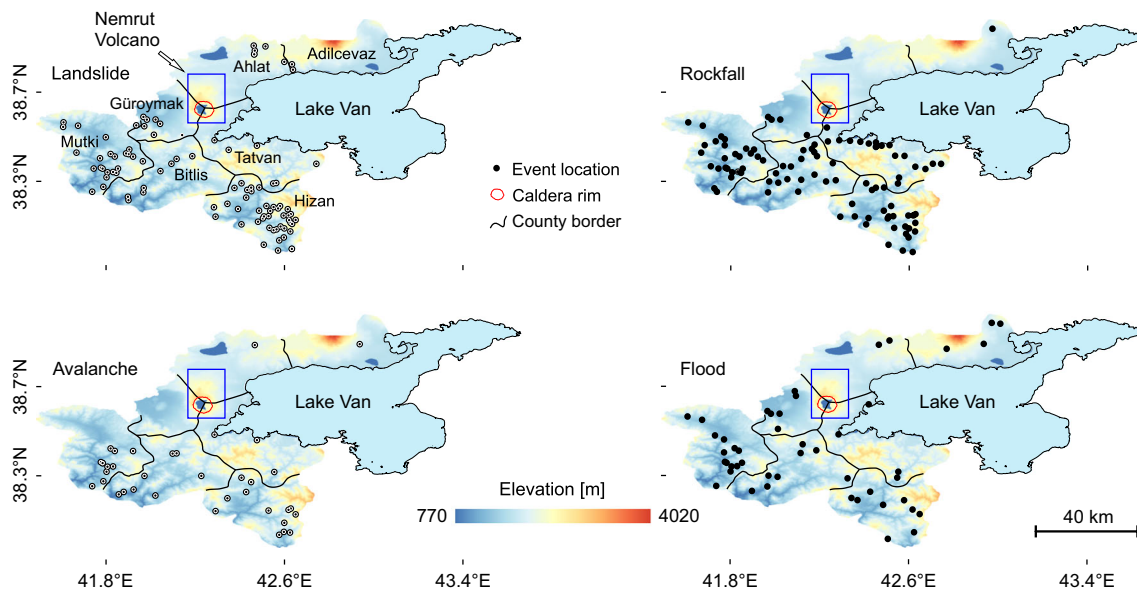


**Fig. 7** Natural hazards of landslide, rockfall, avalanche, and flood events from 1965 to 2010 for Bitlis city. The data set was obtained from Ekinci (2018) and Ekinci et al. (2020b). The figure uses Universal Transverse Mercator projection with WGS 84 datum in 38 Northern Hemisphere Zone

indicating a record of the site and landscape type in the land register, but no conversation practice was specified (to see details, query block: 177, plot: 49, city: Bitlis, county: Tatvan in SAYS (2020)). The information described above implies that the geomorphosite has not been utilized thus far, and its *scientific value* is lacking, so the *key locality* and *scientific knowledge* criteria were scored at 0. Related to the *integrity* of the site, the site is currently quite altered (given a score of 1); the fairy chimneys degraded over time (AA 2015), and the debris was removed (Fig. 12c). The geosite consists of one type of element, so it was scored at 0 for *geological diversity*. According to its *rarity*, the geosite is of a unique type (given a score of 4). The geomorphosite has no *limitations* for sampling or fieldwork (given a score of 4).

The indicator and total *scientific value* scores of this geosite are given in Table 6 and represented on the graphs in Fig. 8.

### The Rift Zone

One of the latest volcanism events in the studied region is the formation of the rift zone (Fig. 2). It includes highly unusual geosites with lithologic elements such as basalt and rhyolite flows with enclaves (geosites 6, 7, 8, and 9). The N-S elongated rift zone is very clear from the vicinity of Kantaşı Hill (Figs. 2, 4, 13a, and 13b); Kantaşı Hill (Nemrutbaşı Dome, geosite 8) is a part of the rift zone (Dome 8 in Figs. 4, 13c, 14a, and b). The geosites in this region (6, 7, 8, and 9) are indicators of the historical events that occurred in 1441–1597 AD (Şerefhan 1597; Karakhanian et al. 2002; Aydar et al. 2003)

**Table 6** Scores for indicators, weights, and total SV for the geosites

Indicator scores/weighted scores <sup>a</sup>	Kirkor dome complex	Kale dome	The caldera		The lakes	Nemrut camels	The rift zone
			The caldera base	The caldera wall			
Representativeness	4/1.2	4/1.2	4/1.2	4/1.2	4/1.2	4/1.2	4/1.2
Key locality	1/0.2	1/0.2	2/0.4	2/0.4	2/0.4	0/0	1/0.2
Scientific knowledge	4/0.2	4/0.2	4/0.2	4/0.2	4/0.2	0/0	4/0.2
Integrity	4/0.6	4/0.6	4/0.6	4/0.6	4/0.6	1/0.15	4/0.6
Geological diversity	0/0	0/0	4/0.2	4/0.2	0/0	0/0	0/0
Rarity	1/0.15	4/0.6	4/0.6	4/0.6	4/0.6	4/0.6	4/0.6
Use limitations	4/0.4	4/0.4	4/0.4	4/0.4	4/0.4	4/0.4	4/0.4
<b>Total SV score<sup>b</sup></b>	<b>2.75</b>	<b>3.20</b>	<b>3.60</b>	<b>3.60</b>	<b>3.40</b>	<b>2.35</b>	<b>3.20</b>

<sup>a</sup> The weighted scores equal to the product of the grades and the weights given in Table 2 for each geosite

<sup>b</sup> The total geosite SV scores are the sum of the weighted scores for each geosite

**Table 7** Scores for indicators, weights, and total PTU for the geosites

	Indicator scores/weighted scores <sup>a</sup>	Kirkor dome complex	Kale dome	The caldera		The lakes	Nemrut camels	The rift zone
				The caldera base	The caldera wall			
Geo-patrimonial	Vulnerability	4/0.4	4/0.4	1/0.1	1/0.1	1/0.1	1/0.1	4/0.4
	Uniqueness	2/0.2	2/0.2	4/0.4	4/0.4	4/0.4	2/0.2	4/0.4
	Observation Conditions	4/0.2	4/0.2	4/0.2	2/0.1	4/0.2	4/0.2	4/0.2
	Interpretative potential	4/0.4	4/0.4	4/0.4	3/0.3	4/0.4	4/0.4	2/0.2
Socio-economic	Density of population	1/0.05	1/0.05	1/0.05	1/0.05	1/0.05	1/0.05	1/0.05
	Economic level	1/0.05	1/0.05	1/0.05	1/0.05	1/0.05	1/0.05	1/0.05
Communication	Accessibility	2/0.2	2/0.2	2/0.2	2/0.2	2/0.2	2/0.2	2/0.2
	Proximity of recreational areas	4/0.2	4/0.2	4/0.2	4/0.2	4/0.2	4/0.2	4/0.2
Precaution	Limitations	4/0.2	4/0.2	4/0.2	4/0.2	4/0.2	4/0.2	4/0.2
	Safety	0/0	0/0	0/0	0/0	0/0	4/0.4	0/0
Logistic	Logistic	4/0.2	4/0.2	3/0.15	3/0.15	3/0.15	4/0.2	3/0.15
Bio-cultural	Association with other values	0/0	0/0	4/0.2	4/0.2	4/0.2	0/0	4/0.2
Aesthetic	Scenery	0/0	0/0	3/0.45	3/0.45	3/0.45	0/0	0/0
	<b>Total PTU score<sup>b</sup></b>	<b>2.1</b>	<b>2.1</b>	<b>2.6</b>	<b>2.4</b>	<b>2.6</b>	<b>2.2</b>	<b>2.25</b>

<sup>a</sup> The weighted scores equal to the product of the grades and the weights given in Table 5 for each geosite

<sup>b</sup> The total geosite PTU scores are the sum of the weighted scores for each geosite

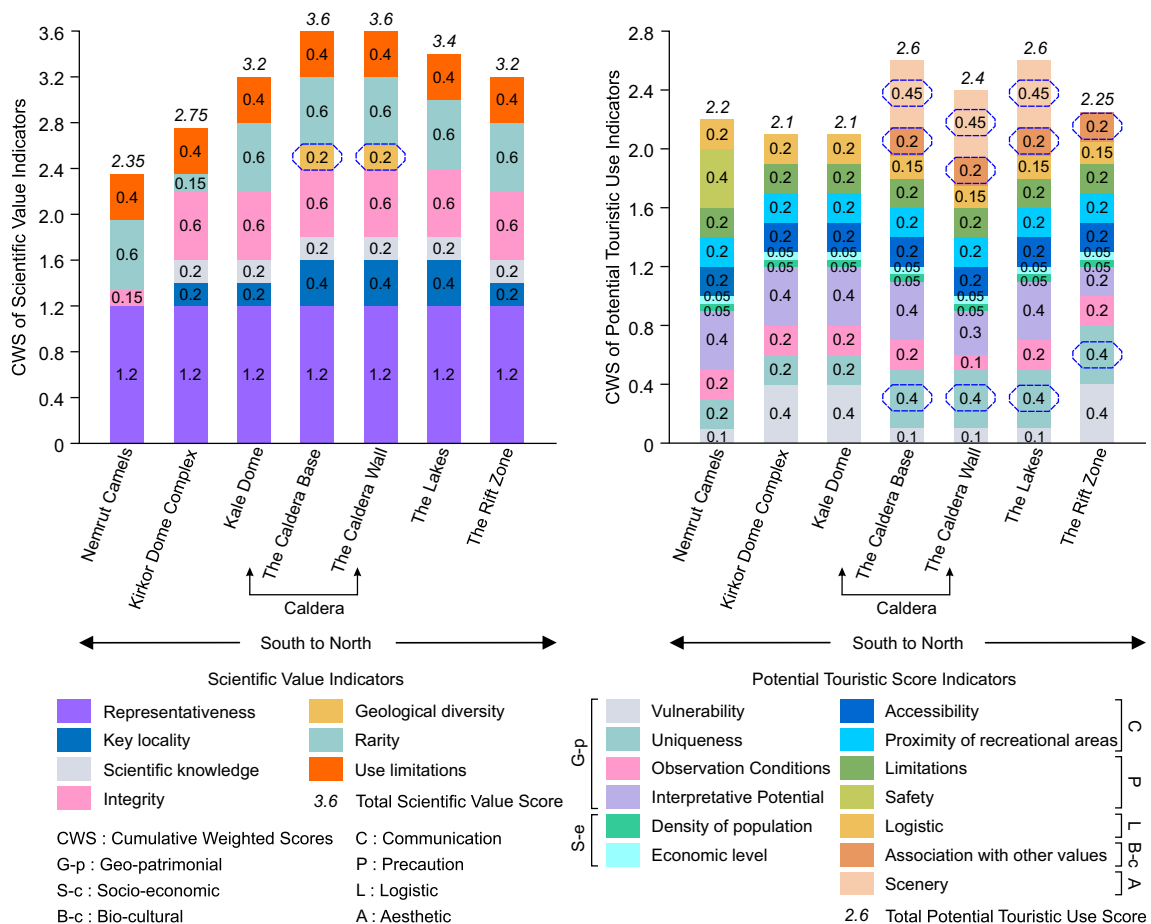


**Fig. 8** The graph of *scientific value* and *potential touristic use* total and indicator scores

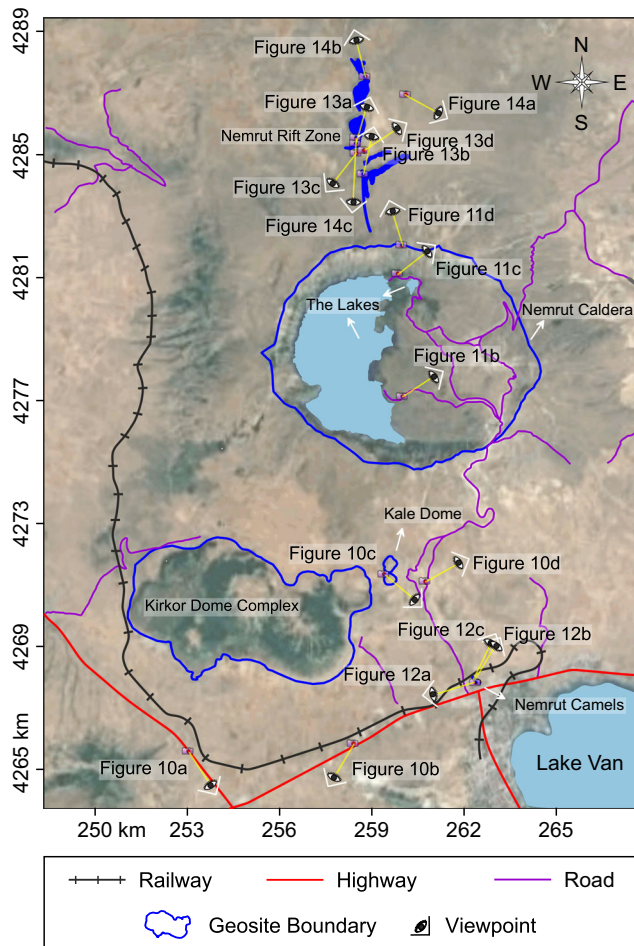


**Fig. 9** Snapshots of Nemrut Volcano geosites. Photo symbols on the map indicate coordinates of snapshots given their images in Figs. 10, 11, 12, 13, and 14. Viewpoint symbols on the map are to show heading angles of snapshots. Heading angle is based on compass directions toward true North. Yellow lines are to separate symbols on the map so that they do not overlap each other. The snapshot view directions can be shown interactively in the Supplementary Information. The figure uses Universal Transverse Mercator projection with WGS 84 datum in 38 Northern Hemisphere Zone

during the post-caldera stage (Figs. 13c, d, and 14) and are linked to myths. The myths (folk tales) narrate distorted realities not only of the caldera and the lakes formed as a result of the god's wrath against King Nemruz but also of the historical volcanic events of 1441–1597 AD. That is, according to the myths, the rift zone formed with the death of the King, as his blood flowed and coagulated (Karaoğlu and Kılıç 2017). The significance of these sites is connected to their stratigraphic setting in relation to the latest volcanism stage (Karaoğlu et al. 2005; Ulusoy et al. 2008, 2012; Çubukçu et al. 2012). Consequently, the sites were scored at 4 for the *representativeness* criterion. According to the *key locality* criterion, the sites could be used at the national (regional) level (given a score of 1) because the rift zone reveals the youngest activity in the Eastern Anatolian region (Yılmaz et al. 1998), with a localized extension between the Otluk fault (OtF in Fig.

4) in the north and the Bitlis–Zagros suture zone (thrust fault in Fig. 4) in the south. The international scientific papers that have been published about the stratigraphic significance of this rift zone caused the sites to be scored at 4 for the *scientific knowledge* criterion. The geodiversity elements are very well preserved (Figs. 13 and 14) because of the rural conditions, linked to the *integrity* of the sites (given a score of 4). The *geological diversity* only includes the lithological type (basalt and rhyolite flows), so this indicator was scored at 0. Regarding the *rarity* criterion, the geosites comprise a single-type lithology connected to lava flows and fountains in the rift zone (given a score of 4). The geosites have no limitations for sampling or fieldwork (given a score of 4). The indicator and total *scientific value* scores of these geosites are given in Table 6 and on the graphs given in Fig. 8.

### Geotourism Assessment of Nemrut Volcano Geosites

The geosites shown in Fig. 2 were quantified by the perception view based on the geo-patrimonial interest criteria (*vulnerability* in Table 3; *uniqueness*, *observation conditions*, and *interpretative potential* in Table 4). Additionally, the conditions of nearby settlement(s) (Bitlis and/or Tatvan in Fig. 2) were also quantified. The conditions were grouped as auxiliary criteria and subgrouped based on socio-economic indicators (*population density* in Table 3 and *economic level* in Table 4), communication indicators (*accessibility* in Table 3 and *proximity of recreational areas* in Table 4), precaution (*limitations* and *safety* in Table 3), logistic factors (Table 3), bio-cultural features (*association with other values* in Table 3) and aesthetic value (*scenery* in Table 3). A geotourism assessment of the geosites at Nemrut volcano is given for each indicator in Table 7 along with the total *potential touristic use* scores of the geosites. The scores are also represented on the graphs shown in Fig. 8.

### Assessment of Geo-Patrimonial Criteria

No traces of deterioration are observed in the geodiversity elements at the sites due to human activities, excluding the site of the Nemrut camels (geosite 5 in Fig. 12). The caldera and the lakes are also prone to potential deterioration of all geodiversity attributes, so they are protected as a Ramsar site (Ramsar 2019) and as a natural park by the MAF (2020). The domes and the rift zone are rural sites, so they have no sign of potential deterioration. Hence, the sites were scored at 1 (the Nemrut camels, the caldera and the lakes) and 4 (the domes and the rift zone) for the *vulnerability* criterion (Table 7; Fig. 8).

Nemrut volcano has caldera-formation and caldera-lithology assets that are common in the region because

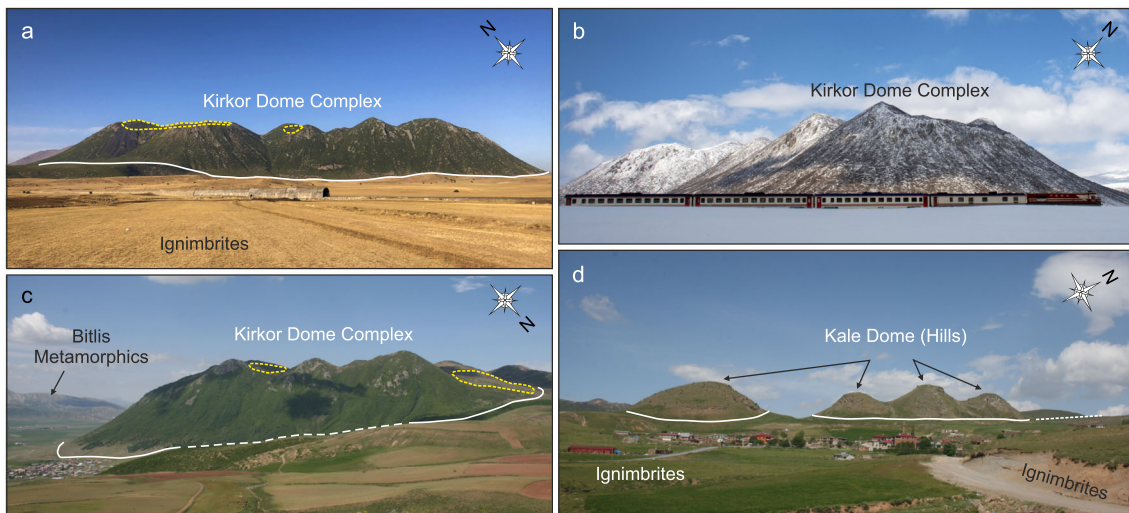


**Fig. 10** Dome type geosites (geomorphosites) around Nemrut Volcano; **a** A picture of Kirkor dome complex (the geosite 1 in Fig. 2) from the SW-NE direction. The flat terrain-dome boundary (the white line) depicts the geosite boundary. The dashed yellow lines mark remnant ignimbrite deposits. **b** A view of Kirkor dome from SE-NW direction in winter. **c** A view of the dome from the hilly side and the SW-NE direction. The dashed white line is the projection of the geosite boundary passing through the unseen valley from the standpoint. **d** A picture of Kale dome

(hills) from the SE-NW direction (geosite 2 in Fig. 2). The hills are linear and protrude sharply on ignimbrite deposit plain. The geosite boundaries are sketched with the white line. The dashed line at the left-hand side of the picture is the inferred fault which runs from Kale dome (numbered with 6 in Fig. 4) to the southern topographic rim in N-S direction on Fig. 4. The locations and viewpoints of the snapshots are given in Fig. 9. The snapshot view directions can be shown interactively in the Supplementary Information

eruptive events also occurred at other Quaternary volcanoes (Süphan, Girekol, Tendürek, and Ararat) within Eastern Anatolia over time. However, Nemrut volcano experienced the most recent volcanic event in 1441-1597 AD (Şerefhan 1597; Karakhanian et al. 2002; Aydar et al. 2003); this event was linked to rift activity compared to Quaternary volcanoes within Eastern Anatolia. That is, the Süphan and Girekol volcanoes experienced the latest eruptive events at 60 ka (Özdemir and Güleç 2014) and  $360 \pm 60$  ka (Lebedev et al. 2010), respectively. Tendürek Volcano contains no products younger than  $25 \pm 30$  ka (Lebedev et al. 2016), but a 1855 eruption of gas and ash (no volcanic products were observed on the terrain) was confirmed by historical records (Karakhanian et al. 2002). The latest activity of Ararat Mountain was an eruptive cloud in 1840 confirmed by historical records (Karakhanian et al. 2002). The latest event occurring at Nemrut volcano represents a rare asset at both the Eastern Anatolian and Continental European scales when compared to the EGN geopark list (the argument in the next main section), so the caldera, lakes and rift zone were scored at 4 for *uniqueness*. This does not mean that the other Quaternary volcanoes within the region do not have unique elements, as they have not yet been studied or published in an assessment scheme. The domes and Nemrut camels (fairy chimneys) are common assets in the region but are uncommon in other parts of the country. Thus, the domes and Nemrut camels were scored at 2 for *uniqueness* (Table 7; Fig. 8). The fairy chimneys, which are conical-columnar erosional landforms, exceed 10 m in height in the Cappadocia region

of Central Anatolia Volcanic Province (Doğan et al. 2019). The Nemrut camels (fairy chimneys) in Eastern Anatolia Volcanic Province reach approximately 5 m in height.

The caldera consists of geomorphologic elements at its base (Fig. 11a) and structural elements on its wall (Fig. 11a, b). The caldera base and the lakes are easily observable and explanatory for laypeople. The caldera wall involves obstacles in terms of the observation of all geo-features, so laypeople will need some background in geology. The *observational conditions* and *interpretative potential* of the caldera base and the lakes were scored at 4, but the caldera wall was scored at 2 and 3 for its *observational conditions* and *interpretative potential criteria*, respectively (Table 7; Fig. 8). The domes and Nemrut camels can be observed clearly, and laypeople do not need a geological background to interpret these sites (given a score of 4 for *observational conditions* and *interpretative potential*). The rift zone is a lithological geosite, and it is not easy to define the volcanic products in this geosite, but the features are visible (given a score of 4 for *observational conditions*). A solid geological background is necessary for a layperson to interpret the eruptive rocks (given a score of 2 for *interpretative potential*). These scores are given in Table 7 and on the graphs provided in Fig. 8.

**Assessment of Auxiliary Criteria**

The geosites are located next to Bitlis city and Tatvan County (Fig. 2). For the socioeconomic indicators, the *population density* of Bitlis was  $49.58/\text{km}^2$  in 2019 (TSI 2020), so the

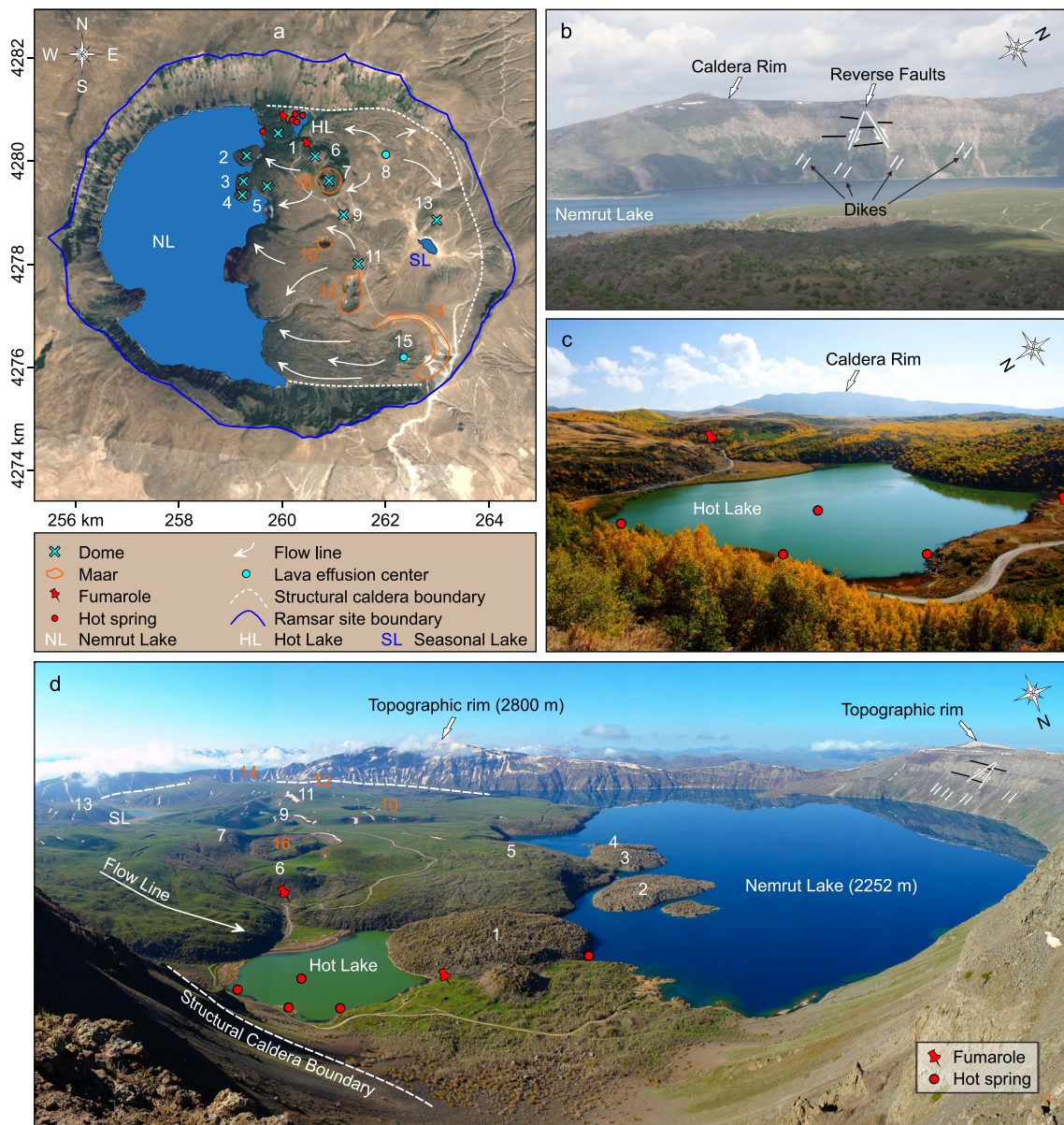


**Fig. 11** Structural (the caldera wall with dikes, reverse faults, and caldera boundary), geomorphologic (domes, lava effusion centers, maars), and hydrologic (Nemrut Lake or cold lake and hot lake with fumaroles and hot springs) geosite elements; **a** The map view of Nemrut Caldera and its geosite elements (the geosites 3 and 4 in Fig. 2). The geosite features are overlaid onto a Google Earth™ image. The blue line coincides with almost the topographic (caldera) rim. It designates the Ramsar (2019) site and natural monument boundary of MAF (2020). **b** A snapshot of the western caldera wall from the SE-NW direction (geosite 3 in Fig. 2). On the wall, reverse faults and dikes cutting trachyte and comendite were drawn (see the western wall of the caldera in Fig. 4). **c** Picturesque view of the hot lake from the NW SE direction. The spatial position of the lake is

shown in Fig. 11a. Fumaroles and hot springs outlets are seen with red dots and pushpins (geosite 4 in Fig. 2). **d** The panoramic view of the caldera from NE-SW direction with the geodiversity features. Some white (dome) and orange (maar) numbers were added from the standpoint of the picture. The dashed white lines are the structural caldera boundary (map view in Fig. 11a) which designates the boundary between the accumulated mass into the caldera and the caldera wall. The reverse faults and dikes (Fig. 11b) drawn with white lines can be seen on the western caldera wall in Fig. 11d. Nemrut (cold) Lake is wholly seen in the panoramic picture (geosite 4 in Fig. 2). The locations and viewpoints of the snapshots are given in Fig. 9. The snapshot view directions can be shown interactively in the Supplementary Information

geosites were scored at 1. This population density does not support geopark development, so the potential for external visitors is crucial. The *economic level* criterion was quantified based on household income, as shown in Table 4. This term includes the monetary value obtained by one (per capita) or

more people living in the same dwelling in a given time. Consequently, the *economic level* (Table 4) was assessed as the GDP per capita (\$). The GDP per capita is an acronym for the per-capita gross domestic product and is a monetary measure of the market value of all final goods and services

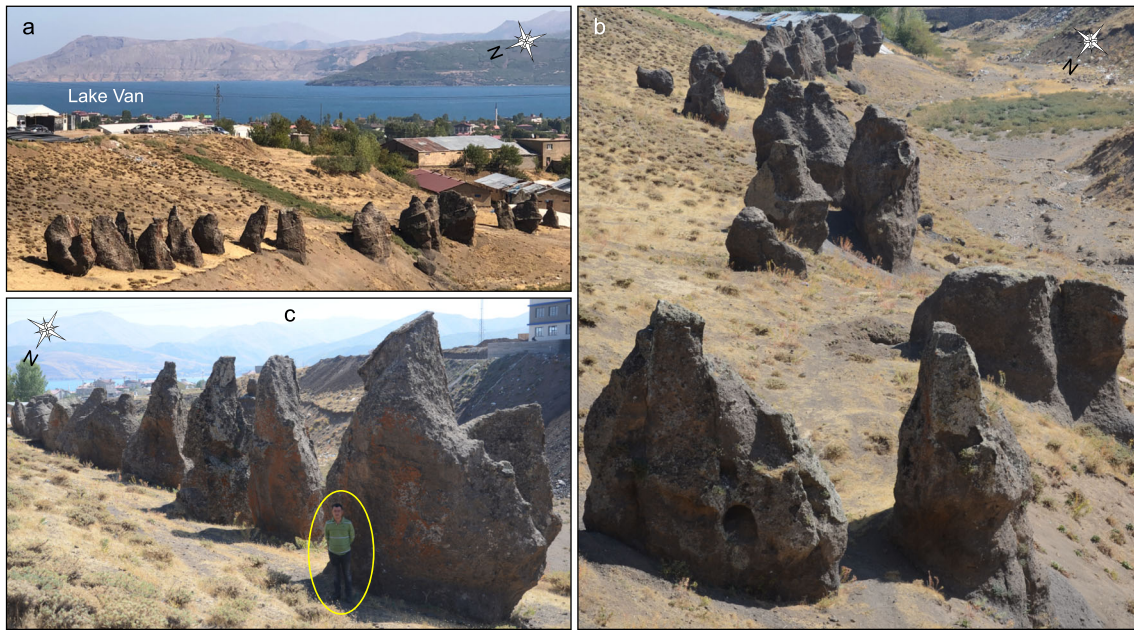


**Fig. 12** An unusual geomorphologic geosite within the erosional realms of Nemrut ignimbrite known as Nemrut Camels (the geosite 5 in Fig. 2). **a** The scenery of the hilly side of Nemrut Camels from NW-SE direction. Urbanization is seen on the opposite hilly side and most probably threatens the event of the camels. **b** Different view of the camels along the river bed from NW-SE direction. **c** Relative size of Nemrut Camels

and debris in the river bed from NW-SE direction. The presence of one of the co-authors marked with the yellow oval on the picture specifies the scale. The locations and viewpoints of the snapshots are given in Fig. 9. The snapshot view directions can be shown interactively in the Supplementary Information

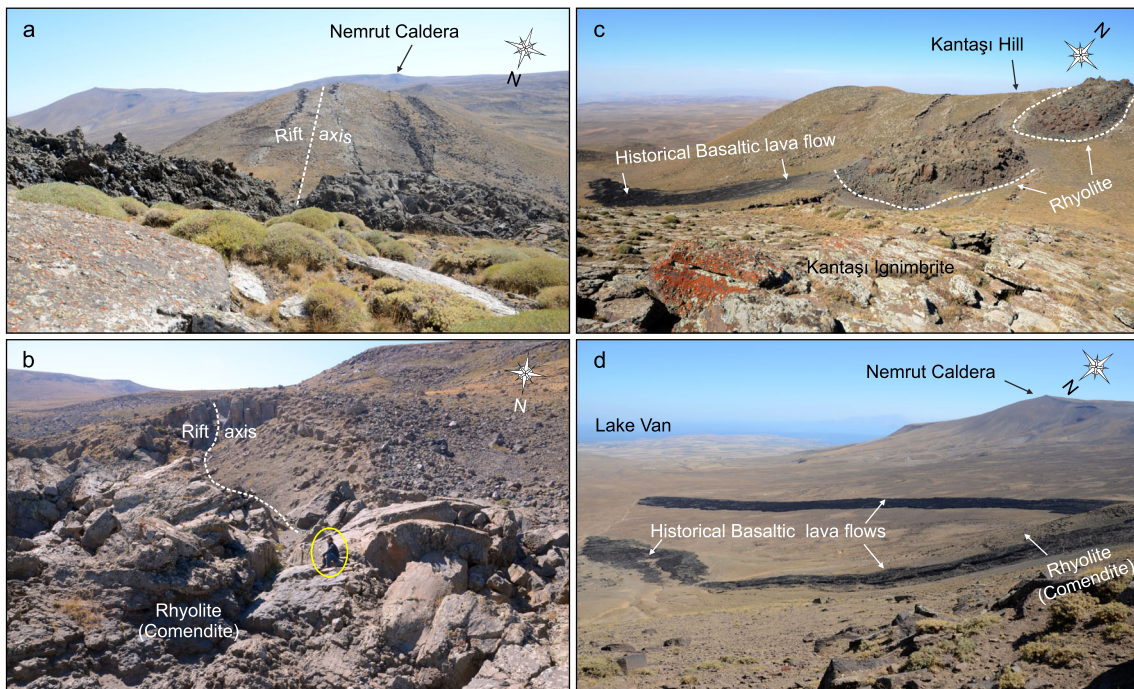


**Fig. 13** Unique lithologic geosites of the Nemrut Rift Zone (geosites 6 and 7 in Fig. 2) referring to the historical events of 1441–1597 AD; **a** Nemrut rift zone axis (geosite 7 in Fig. 2) at the south of Kantası hill (Nemrutbaşı dome) lies to the northern end of the caldera at N-S elongation. Nemrut Caldera rim is on the horizon. Dark-coloured rocks on Kantası hill are comendite type (rhyolite) from 1441 to 1597 AD historical lava flows. The snapshot was taken from NW-SE direction. **b** A view of the extensional nature of the rift zone (geosite 6 in Fig. 2) in the midst of the bulging ground in Fig. 13a and the caldera rim. The presence of one of

the co-authors marked with the yellow oval on the picture specifies the scale. The snapshot was taken from NW-SE direction. **c** A picture of 1441–1597 AD historical basaltic and rhyolitic lava flows (geosite 7 in Fig. 2). The ground is covered with Kantası ignimbrite. The snapshot was taken from SE-NW direction. **d** A picture of 1441–1597 AD historical basaltic lava flow (geosite 6 in Fig. 2). The snapshot was taken from NW-SE direction. The locations and viewpoints of the snapshots are given in Fig. 9. The snapshot view directions can be shown interactively in the Supplementary Information

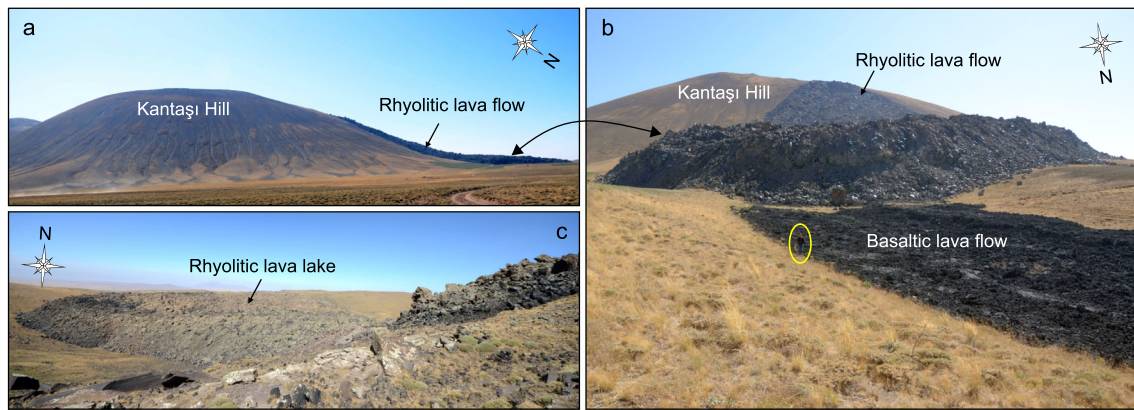


**Fig. 14** Unique lithologic geosites of the Nemrut Rift Zone (geosites 8 and 9 in Fig. 2) referring to the historical events of 1441–1597 AD. **a** Kantaşı Hill (Nemrutbaşı dome) from eastern side and the historical rhyolite flow (geosite 9 in Fig. 2). The snapshot was taken from NE-SW direction. **b** Kantaşı Hill from north view and the expression of bimodal activity comprising historical rhyolitic and basaltic lava flows (geosite 9 in Fig. 2). The snapshot was taken from NE-SW direction. The presence

of one of the co-authors marked with the yellow oval on the picture specifies the scale. **c** The apex view of Kantaşı Hill and the historical rhyolitic lava lake (geosite 8 in Fig. 2). The snapshot was taken from S-N direction. The locations and viewpoints of the snapshots are given in Fig. 9. The snapshot view directions can be shown interactively in the Supplementary Information

produced in a specific period per person (capita) (Economocshelp 2020). The GDP per capita values in Turkey and Bitlis in 2018 were \$9693 and \$3767, respectively (TSI 2020). The GDP value for Bitlis is lower than the national average, so the sites were scored at 1 for the *economic level* criterion (Table 7; Fig. 8).

The road conditions (Fig. 2) necessary for transportation between accommodation and the geosites are partly present. The roads are connected to highways (Fig. 2), but access to the geosites requires a vehicle, not only due to the distances of the geosites from the highways but also due to the unpaved road conditions (*accessibility* scored at 2). A recreational area, a ski sports facility, is located on the southern flank of Nemrut volcano (Fig. 2). The distances from the other geosites were calculated via Google Earth™ with a routine query protocol. The distance from the Kirkor dome complex to the ski sports facility is no less than 20 km (35.6 km). The Kale domes are 14.4 km away from the facility. The Nemrut camels and the rift zone are 10.0 and 53.3 km away from the facility, respectively. These route distances cannot be separately assessed because the Nemrut Volcanic Geopark Project proposal includes all geosites, so it is considered unique. The recreational site is located inside the caldera (Fig. 2), so the *proximity of recreational areas* criterion (Table 4) was scored at 4 for all geosites (Table 7; Fig. 8).

There are no obstructions to the utilization of all geosites by students and tourists to be considered under the limitations criterion (scored at 4). Regarding the *safety* criterion, the rift zone is located more than 50 km away from the emergency services in Tatvan County. All other geosites are located less than 25 km from the emergency services. Mobile network coverage depends on the mobile operator service for subscribers and cellular network technologies (2G-GSM, 3G-UMTS, or 4G-LTE) broadcasting in Turkey. The GSM (the

most common) cellular network map around Nemrut volcano shows void signal areas in and around the geosites in the caldera, lakes, domes, and rift zone (GSMA 2020a, 2020b, 2020c). Unlike the GSM map, the 3G and 4G maps generally cover minor areas, and larger signal voids exist in these maps in and around the geosites of the caldera, the lakes, the rift zone, and the domes (wholly or partly) (GSMA 2020a, 2020b, 2020c). To avoid excessive and uncertain assessments, we chose the indicator or phrase without mobile phone coverage for the geosites of the caldera, the lakes, the domes, and the rift zone. This phrase was not recorded in Brilha (2016), but zero scores are available when necessary. Hence, the geosites (the caldera, the lakes, the domes, and the rift zone) were scored at 0 for the *safety* criterion without accounting for their proximity to emergency services to err on the side of caution (Table 7; Fig. 8). We indicate a methodological gap here and suggest differentiating the mobile phone and emergency service indicators for future scoring. By doing so, the uncertainty resulting from the combined evaluation of the safety regulation indicators would be diminished. The Nemrut camels are located less than 5 km away from emergency services and have mobile phone coverage, so this geosite was given a score of 4 for the *safety* criterion (Table 7; Fig. 8). We strongly recommend in situ emergency services and more widespread mobile phone coverage inside the proposed geopark, especially for the geosites of the caldera, lakes, domes, and rift zone.

The domes and Nemrut camels are located less than 15 km from accommodations and restaurants for 50 people or more (Table 3) in Tatvan County. This county was chosen as the nearest point to the geosites (Fig. 2) with advantages for transportation (ferry routes and highways) rather than Bitlis city, so these geosites were scored at 4. The rift zone is approximately 50 km away from *logistic* features, but Nemrut caldera and the lakes are less than

50 km away. Hence, the remaining geosites were scored at 3 (Table 7; Fig. 8).

There are areas of cultural value (touristic spots) located around the proposed geopark site of Nemrut volcano. The ferry route and the highway linking Tatvan County to Lake Van (Fig. 2) and Van city connect visitors to touristic spots such as Armenian Aghtamar Church (Aghtamar Church 2020), Kef Fortress (Kızmaz 2014, Kef Fortress 2020), Adilcevaz Castle (Kızmaz 2014), and Süphan Dam, a Urartian water work built in 700 BC (Öziş 2015). The distance between the touristic spots and Tatvan County is greater than the distance given in the *association with other values* indicator (Table 3), so the distance grading is outside the parameters of this criterion. Thus, the geosites were scored at 0 (Table 7) except for the caldera and the rift zone because their activities are recorded in historical references (Şerefhan 1597; Karakhanian et al. 2002) and have mythological influences (details and references are presented in the next main section). In addition, the caldera has ecological importance because it is a Ramsar site. Thus, these geosites were scored at 4 (Table 7; Fig. 8).

Nemrut caldera and its lakes are a Ramsar site (Ramsar 2019). The caldera and the lakes are used as tourism destinations, but not regularly, so they were scored at 3 for the *scenery* (aesthetic value) criterion. However, the domes, rift zone, and Nemrut camels are virgin landforms. Hence, they were scored at 0. The rift zone has scenic features, but its *accessibility* score (Table 7; Fig. 8) shows that the road conditions need improvement. The domes represent a potential *scenery* feature, as they can be used to observe landforms in the nearby Nemrut caldera. The caldera, by contrast, not only has potential due to its scenic features but also has the highest *potential touristic use* score due to the lakes (Table 7; Fig. 8).

When geodiversity assets have remarkable aesthetic relevance (especially geomorphological assets), their comparatively high *potential touristic use* scores indicate that they can be appreciated aesthetically with common sense and can be easily understood by people without geoscientific backgrounds (Brilha 2016). As stated earlier, the caldera base (geosite 3) and the lakes (geosite 4), which are geomorphologic and hydrologic landform types, respectively, are remarkable for laypeople. The domes and Nemrut camels do not require a geoscience background either. The statement published by Brilha (2016) did not satisfy all relevant high scores for scientific and educational values. For instance, the Kale dome has the lowest *potential touristic use* score (2.1 in Table 7; Fig. 8) but a high *scientific value* score (3.20 in Table 6; Fig. 8). This means that any value should be chosen diacritically when a geosite is planned within a geopark project or proposed as a geoheritage site. What makes a geosite exceptional depends on the in situ values of the geosite, such as scientific, cultural or aesthetic values for geotourism (Brilha 2018); even so, the principal value must

highlight the *scientific value* (Brilha 2016) of the site, even if its aesthetic aspects are remarkable. Geotourism interest is crucial for utilitarian needs, especially in the case of conserving geodiversity value(s) inside a geopark. As seen in Table 7 and Fig. 8, the aesthetic (*scenery*), bio-cultural (*association with other values*), and geo-patrimonial values (*uniqueness*) of the caldera, lakes, and rift zone provide contrast with the indicator and final output scores. The geo-patrimonial (scientifically oriented values) scores highlight the remarkable aesthetic score, as given in a general statement by Brilha (2016), in addition to the bio-cultural scores shown in Table 7 and Fig. 8. The geotourism (*potential touristic use*) scores might also increase with the effects of improving socio-economic and *accessibility* conditions related to these indicators because of the current low scores in the assessment (Table 7).

### Comparison of the Scientific Value and Geotourism Assessment of Nemrut Volcano Geosites

The *scientific value* scores are higher for the geosites of the caldera (geosite 3) and the lakes (geosite 4) than for the other geosites, as shown in Table 6 and Fig. 8. In detail, the *geological diversity* indicator, a sub-component of the *scientific value*, is highly remarkable for the caldera geosite (0.2) compared to the other geosites (0.0). The aesthetic (*scenery*), bio-cultural (*association with other values*), and geo-patrimonial (*uniqueness*) values of the geosites of the caldera (geosite 3), the lakes (geosite 4), and the rift zone (geosites 6, 7, 8, and 9) contrast with the scores given to for the indicators and the final output of the *potential touristic use*, as seen in Table 7 and Fig. 8. The rest of the auxiliary criteria portray environmental conditions, so they do not vary significantly. In detail, the *uniqueness*, as a geo-patrimonial criterion, bio-cultural (*association with other values*), and aesthetic (*scenery*) scores highly influence the geotourism (*potential touristic use*) scores for the geosites of the caldera, the lakes, and the rift zone compared to the other geosites (Fig. 8). The geo-patrimonial (scientifically oriented values) scores highlight the remarkable aesthetic score, as given in a general statement by Brilha (2016), in addition to the bio-cultural scores shown in Table 7 and Fig. 8. Regardless of the type of geodiversity element that is considered with the geoheritage criteria (outstanding), a site must be assigned high score(s) for economic, scientific, or aesthetic aspects (Brilha 2018). In this study, the highest *scientific value* and *potential touristic use* scores (Fig. 8) were well matched for the caldera (geosite 3) and the lakes (geosite 4). Thus, we propose that Nemrut volcano, especially the geosites of Nemrut caldera and the lakes, has remarkable scientific, cultural, and aesthetic value and supports in situ biotic features to the degree that the geosites of the volcano are considered geopark and geoheritage sites.

## Geopark Value of Nemrut Volcano

We argue the nomination of Nemrut volcano as a geopark and a geoheritage site. The volcano has remarkable value due to its unique geographic-geologic setting compared to volcanic themes in the European Geopark Network together with its own biodiversity and cultural (mythological and auxiliary) values.

The oldest volcanic themes in the EGN were part of ancient orogenesis (Hercynian, Avalonian-Cadomian, and Caledonian) and occurred in continental and Atlantic Europe. These volcanic themes cover 12% of the entire list of EGN (2020). The extinct volcanic themes in the EGN are part of the (pre-)Alpine orogeny or part of extensional basins related to the Alpine orogeny. They occur in continental Europe, except for Cyprus Island, and cover 11% of the EGN list. The active volcanic themes in the EGN represent different geologic settings. Geoparks related to extensional basins linked to the Alpine orogeny can be found in the south eastern passage to continental Europe (Anatolia), apart from Vulkaneifel Geopark (Germany). The Macaronesia and European Arctic regions located far from continental Europe display different volcanic plumbing mechanism(s) related to the hotspot zone in the Atlantic Ocean, the Mid-Atlantic Ridge or the seismic Gloria fault. These volcanic schemes cover 9% of the EGN list. They formed from the Holocene to the present, but present volcanic themes are only found on the Atlantic Ocean front of Europe. The youngest activity in continental Europe among the geoparks in EGN with volcanic themes can be found in the Vulkaneifel Geopark (Germany); this activity is linked to deglaciation unloading and dates to 10,970 years ago (Nowell et al. 2006). The Chaîne des Puys volcanism is the latest activity, having occurred 7000 years ago (Boivin and Thouret 2014), but this volcano is not part of a registered geopark in the EGN. The Kula Geopark, a member of the EGN list, is found in Anatolia, but its volcanism dates to  $4 \pm 2$  ka (Şen et al. 2019). However, Nemrut volcano, a proposed geopark site, exhibits the most recent volcanism, with historical events recorded in 1441–1597 AD (Şerefhan 1597; Karakhanian et al. 2002; Aydar et al. 2003) in Anatolia. This statement about Nemrut caldera was derived from the premises given in the Appendix 1, in which the geoparks with volcanic themes in EGN are listed and grouped by common features based on literature research.

At the stratovolcano, 43 species out of 450 plant species are endemic (Seven et al. 2019). Noteworthy fauna include a species of velvet scoter (*Melanitta fusca*, *M. fusca* in abbreviated form), which is classified as vulnerable according to BirdLife International (2020). *M. fusca* also breeds in the lake(s) of the caldera. Hence, the water bodies (the temporal lakes, Nemrut Lake and the hot lake shown in Fig. 2) are considered a Ramsar site based on the first criterion of Ramsar (2019), which accepts the wetland as a rare example within the

biogeographical criteria. We extend this acceptance to the second criterion, which is linked logically to the first criterion (Ramsar 2019). This measure is connected to wetlands (the caldera lake(s) herein) that support vulnerable and endangered species (*M. fusca* and endemic plants).

The myth (Şerefhan 1597; Karaoğlu and Kılıç 2017) narrates the death of King Nemruz as a result of god's wrath. This is a local myth that comprises other terms that are directly linked to distorted realities of Nemrut volcanism (associated with Nemrut caldera, Nemrut camels, and the rift zone). Archaic versions of mythological resources reach broader geographic realms (Eastern Anatolia and Mesopotamia). Gadjimuradov and Schmoeckel (2005) indicated a hero-god "Ninurta" in Mesopotamia (Akkadians and Sumerians), illustrated with flames. Except for the god, the etymological connection between Nemrut and an Assyrian king "Ninurta" was established in their work. The Assyrian kingdom (Mesopotamian) campaigned in the territory of the Urartian Kingdom (Eastern Anatolian) from 1275 to 840 BC and from 840 to 612 BC (Encyclopædia Britannica 2020a), when Assyria was ruled by Tukulti-Ninurta I (circa 1243 to 1207 BC) and by Tukulti-Ninurta II (circa 890 to 884 BC) (Encyclopædia Britannica 2020b, 2020c). The second phase of Assyrian invasion matched well with the latest phreatomagmatic/phreatic activity ( $787 \pm 25$  and  $657 \pm 24$  BC) of the Nemrut stratovolcano (Ulusoy et al. 2012), so the myth may reflect the brutality (corresponding to the ash eruptions and linked volcanic-seismic events) of the volcanic eruptions. In summary, the religious-etymological continuity of Ninurta from a hero-god to an Assyrian king with his divine rulership may be linked to a distorted reality of the latest Nemrut ash eruptions. Afterwards, the myth could have been reduced to the local folkloric scale at which it was written in Şerefhan (1597).

Areas of cultural value (touristic spots) are located around the Nemrut Volcanic Geopark Project. The ferry route and the highways linking Tatvan County to Lake Van (Fig. 2) and Van city connect visitors to touristic spots such as Armenian Aghtamar Church (Aghtamar Church 2020), Kef Fortress (Kızmaz 2014, Kef Fortress 2020), Adilcevaz Castle (Kızmaz 2014) and Süphan Dam, a Urartian water work built 700 BC (Öziş 2015). In prehistoric times, the location near the trachyte outcrops on the eastern flank of Nemrut caldera (Fig. 4) and the area inside Nemrut caldera could have been used as sources of raw obsidian material (Robin et al. 2016; Frahm 2020). However, no archaeological ruins have been reported in the studied publications. Springs in the vicinity of the caldera and the cold lake at the base of the caldera are also interesting for researchers due to the potential exploitation of these water resources. The estimated potential water obtained by dropping the level of the cold lake by 1 m equals a water volume of  $12.4 \times 10^6$  m<sup>3</sup>; this value corresponds to the water consumption of nearly 350,000 people annually (Kurttaş and

Tezcan 2017). The cold lake at the caldera base is a part of the Ramsar site (Ramsar 2019). Hence, the lake has not yet been exploited. Kurttaş and Tezcan (2017) noted that the water capacity of the cold lake could be used in serious conditions of water scarcity.

A suggested tourist route plan for Nemrut volcano, a proposed geopark site, is given in Fig. 15. By using highways and roads from nearby cities and counties (Fig. 15), potential visitors can reach the observation points (Op). The first two destinations (Op1 and Op2 in Fig. 15) are the observation points of the Kirkor Dome Complex (geosite 1) and Kale domes (geosite 2), respectively, and depict the pre-caldera stage of Nemrut volcanism. A road should be constructed between Op1 and Op2 (the road shown by green dots in Fig. 15). Op3 is the destination for the erosional realms known as the Nemrut camels (geosite 5) and depicts the widespread volcanism produced during the syn-caldera stage. The road conditions from Op2 to Op3 should be improved (the road shown with a green line in Fig. 15). Destination Op4 is a sightseeing point for the observation of the landscape view, including Lake Van and the south-eastern flanks of Nemrut caldera and the domes (Fig. 15). Points Op5 and Op6 are observation points for the caldera, including the caldera wall and caldera base (geosite 3) and the lakes (geosite 4), respectively. Op5 is selected to represent the caldera formation during the syn-caldera stage. Destination Op6 is selected to represent the lakes (geosite 4) depicting hydrologic assets in the caldera. The road from Op3 to Op6 is open for use (the road shown with a magenta line in Fig. 15). The destinations of Op7, Op8, and Op9 are suggested for the rift zone (geosites 6, 7, 8, and 9) and depict the post-caldera stage of Nemrut volcanism. The road from Op6 to Op9 is partially open (the road shown with a magenta line in Fig. 15), but the other sections of the road suggested for these points should be improved and constructed (the roads shown with green dots and with a green line in Fig. 15). The tourist route for the proposed Nemrut volcano geopark site was chosen on land surfaces with slopes lower than 30% because slopes greater than or equal to 30% comprise fault scarps (Gedikpınar rise in Fig. 6a), collapse structures (caldera walls), or slump structures developed in the ignimbrites (Fig. 6a).

### Conclusions

This paper attempts to assess the geosites of Nemrut volcano and proposes these areas as a geopark and geoheritage site. Despite knowing the geologic significance of this region, no geopark project has been initiated by the local authorities thus far. The Nemrut Volcano Geopark Project should be planned according to a utilitarian-scientific base oriented towards specific tourism events (geotourism). The method used in this study reveals that the *geological diversity, rarity, bio-cultural,*

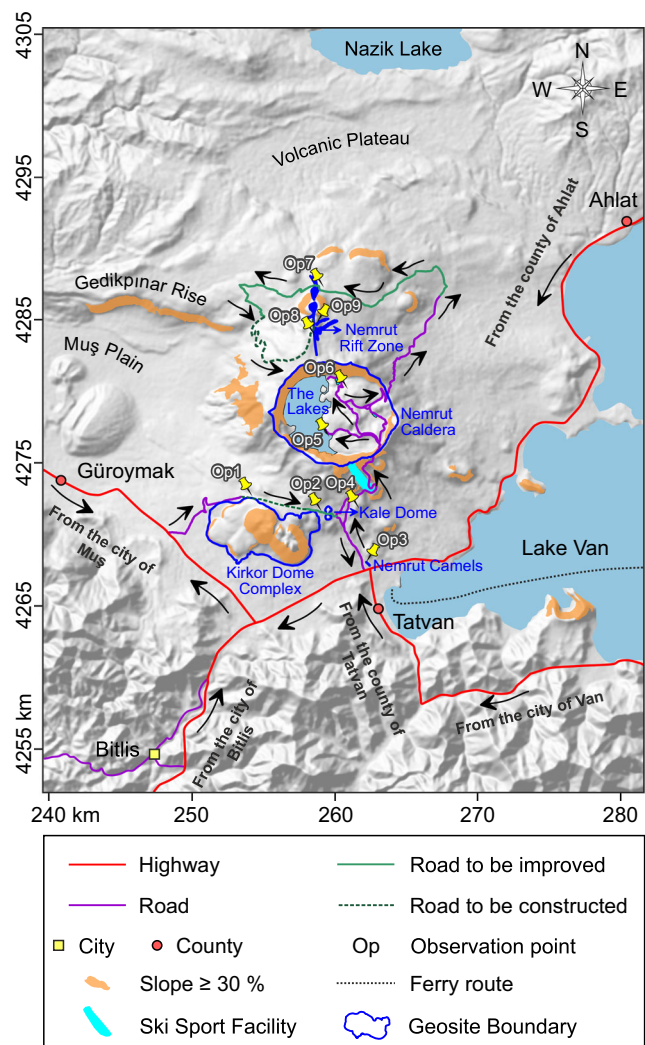


**Fig. 15** The suggested tourist route plan for the geopark site of Nemrut Volcano. The figure uses Universal Transverse Mercator projection with WGS 84 datum in 38 Northern Hemisphere Zone

*uniqueness, and aesthetic* criteria of the region encourage geotourism activities relevant for geopark development. Railway and highway transportation in Bitlis city and Tatvan County are also advantageous for reaching the proposed geopark. Tatvan County and Bitlis city can be easily reached from the Muş and Van airports.

The following improvements are recommended to make the geotourism facility more feasible:

- Ferry routes can be used as an optional transportation route from Van city to Tatvan County.
- Pedestrian paths and roads to the geosites should be improved or constructed for visitors.
- Accommodation services with the capacity for overnight or longer stays based on tourism operation licences are present in Tatvan County. However, the capacity for such services should be increased for national and international visitors.

- Hotels in Tatvan County should provide transportation services to the Nemrut stratovolcano and nearby areas.
- Local people should be educated about tourism guidance to support the local economy.
- Mobile phone coverage inside the proposed geopark should be increased to ensure the availability of in situ emergency services.
- Mobile phone coverage should be used for warning systems in cases of natural hazard occurrences around the proposed geopark.
- The Nemrut volcano geopark should be popularized through leaflets, websites, conferences, and exhibitions.

## Appendix 1 Volcanic Themes in the European Geopark Network and Nemrut caldera

This eclectic nature of the intersection between cultural value and volcanic activity is unique among the geoparks in the European Geopark Network, where the volcanic themes in geographic-geologic settings can be described as ancient, extinct, and active volcanism, in contrast with the proposed geopark site of Nemrut Volcano below. Geoparks with volcanic themes registered in the EGU are described case-by-case and then grouped (by premise) into their relevant geologic setting and geologic age order. The last paragraph in this manuscript is a conclusion statement about Nemrut caldera that was derived from inductive-based premises and the caldera's unique bio-cultural assets.

Only 32% of the current EGN comprises volcanic themes (EGN 2020). The contexts of these volcanic themes were divided into ancient, extinct, and active volcanism herein. Ancient volcanism is recorded in a stratigraphic setting and does not overlap with current plate boundaries (Wood 2009) or is cut off from its magma source(s). These sites are related to ancient (Palaeozoic) orogenies (Avalonian-Cadomian, Caledonian, and Hercynian). Another categorical definition includes extinct volcanoes that are linked to current plate boundaries, Cenozoic deformation belts (herein, the Alpine orogeny), or the Tethyan Ocean; the volcanism at these sites ceased in geologic times (herein, in the Triassic period and Oligocene, Miocene, and Pleistocene epochs). These volcanoes are not expected to become active again on a comparable time scale, but it is not claimed that this extinct volcano type cannot erupt again on the geologic timescale (millions of years). Active volcanism in the Quaternary period encompasses eruption events occurring at present or within recorded history (4360 BC to the present day) according to the US National Oceanic and Atmospheric Administration (NOAA 2020). A more comprehensive context deals only with active volcanoes, with eruption events that have occurred within approximately the last 10,000 years (Holocene epoch) based

on the Smithsonian Institution Global Volcanism Program (SIGVP 2013). The geoparks with active volcanic themes within the Holocene epoch form 9% of the entire list of EGN (2020). Ancient and extinct volcanic themes comprise 12% and 11% of the EGN list, respectively.

The oldest ancient volcanic remnants linked to ancient orogens among the EGNs within continental Europe are Geopark Beaujolais in France, Sesia-Val Grande Geopark in Italy, and Bohemian Paradise Geopark in the Czech Republic. Geopark Beaujolais includes volcanic outputs resulting from the Hercynian (Variscan) orogeny (BUGG 2020) and dating to the Devonian to Carboniferous periods (430–330 Ma) in a volcanic archipelago (GB 2020). The volcanic caldera of the Sesia supervolcano erupted in the Permian period (280 Ma) and is visible at the Sesia-Val Grande Geopark (Selvaggio et al. 2016; SVG 2020). The Bohemian Paradise Geopark (BPG 2020) exhibits the intense volcanism products of continental intermontane basins associated with the Variscan orogeny dated to 360–260 Ma in the Permo-Carboniferous period (Ulrych et al. 2006) and recurrent volcanism in the Cretaceous period (79 Ma) to the Pleistocene epoch (0.26 Ma) via pre-existing Variscan-associated weakness zones (Ulrych et al. 2011). Outside of continental Europe, the oldest ancient volcanic themes related to ancient orogens on the EGN list are located in Atlantic Europe. Geoparks in Wales-UK (GeoMôn Geopark), Scotland-UK (Shetland Geopark), and the UK (North Pennines AONB European Geopark) embody these volcanic themes. The GeoMôn Geopark includes pillow lava linked to arc-related magmatism during the Precambrian (630–570 Mya) associated with the Avalonian-Cadomian orogeny (Linnemann et al. 2007), forming at a Precambrian constructive plate margin that is part of Avalonia (EGN 2020; Murphy et al. 2019). The Shetland Geopark exposes the flank of a stratovolcano that was active during the Caledonian orogeny (GSL 2020), mainly between the late Cambrian and mid-Devonian (490–390 Ma). The North Pennines Geopark has an escarpment that is a volcanic remnant from 480 Ma (EGN 2020; NP 2020). The volcanic material was part of the Iapetus Ocean that subducted during the Caledonian orogeny (Lawrence et al. 2004). The relatively younger (extinct and active) volcanic themes are located across all geographic regions of Europe and are described as follows.

The Geopark Vis Arhipelago (Croatia) displays volcanic occurrences (GVA 2020a) belonging to geo-events of the pre-Alpine orogeny. The volcanic rocks in this geopark are from a volcanogenic-sedimentary-evaporitic complex of Triassic age: the Adriatic Carbonate Platform sequence (Vlahović et al. 2005; Lozić et al. 2012). The complex developed along the Gondwanan margin through the accumulation of siliciclastic-carbonate deposits (Vlahović et al. 2005) and volcanism (Middle Triassic, 247–237 Ma), linked to the partial break-up or drifting of Gondwana and Adria (Vlahović et al. 2005; GVA 2020b). The Troodos Geopark (Cyprus

Island) comprises geosites on the hills and flanks of the Troodos mountain range consisting of ophiolites (TG 2020) known as members of the Troodos complex, dating to 90–92 Ma in the Late Cretaceous (Ring and Pantazides 2019). This complex includes different types of rocks with ophiolitic compositions. One of these rock types is a volcanic complex of pillow lavas and basalt with dikes (TG 2020; GMC 1979). The ophiolites are slices originating from the Late Cretaceous Neo-Tethyan oceanic lithosphere and are linked to the closure of the southern branch of the Neo-Tethys Ocean (Morag et al. 2016). The Troodos complex formed by spreading above the (pre-Alpine orogeny) African and Eurasian plates in the Cretaceous (Ring and Pantazides 2019) and was uplifted (pre-Alpine orogeny) by the collision between these plates (TUGG 2020). Romania (Hateg Country Dinosaurs Geopark) and Hungary-Slovakia (Novohrad–Nograd Geopark) contain volcanism with paleohabitats in continental Europe; the volcanic themes of these geoparks are dated to 72–65 Ma (Late Cretaceous) and 30 Ma (Oligocene), respectively (EGN 2020). The joint geopark in Austria-Slovenia (Karavanke/Karawanken) represents the Smrekovec Volcanic Complex of the Upper Oligocene (ca. 28–23 Ma) and is related to the initial extensional evolution stage of the Pannonian Basin; this stage resulted in continental escape from the collision zone (uplift of the Alps) in the Late Oligocene to Neogene (Kralj 2012; KKG 2020). The Bakony-Balaton (Hungary) geopark in continental Europe has emblematic volcanic remnants (maar, dome and caldera remnants) from calc-alkaline volcanism related to the subduction-collision processes of the Pannonian Basin, which preceded by the closure of two oceanic realms (the Triassic-Cretaceous Neotethys and Middle Jurassic–Paleogene Alpine Tethys Oceans), Miocene syn-rift extension and post-rift basin evolution (Pánisová et al. 2018). The Tethys was formerly an ocean before the Alps (Alp Mountain chain, the outcome of the Alpine orogeny) were uplifted as a result of the collision. The volcanic themes of the Bakony-Balaton Geopark represent late Miocene volcanism dated to 8 Ma (BBG 2020). Papuk Geopark (Croatia) is known for its famous volcanic exposures of columnar jointing in the Rupnica geosite (PGG 2020; Balen and Petrinc 2014); this site is found in the Pannonian Basin. This volcanic exposure is correlated with basin evolution developing from the opening and subsequent closure of the Triassic-Cretaceous Neotethys and Middle Jurassic–Paleogene Alpine Tethys Oceans together with extensional magmatism in the Miocene connected to volcanic successions dated to 22 to 17 Ma in the Dinarides (Balázs et al. 2016). The geopark and Rupnica geosite therein occur in the Dinaride region, whereas the ages of the nearby Rupnica geosite and the Miocene extension of the basin are controversial (reported as 75–32 Ma in Pamić (1991)). Hence, the inference of age is related to the two quite different regional evolutionary settings (pre-Alpine and Alpine) in the basin

(Balen and Petrinc 2014). The Swabian Alps Geopark (Germany) contains volcanic remains of a crater (Hoewenegg erupted 10 Ma in the Miocene) and a maar (Randeck formed 17–20 Ma in the Miocene), elements of Hegau Volcanism at the Rhine Graben rift linked to intra-plate activity in the Alpine orogenic belt (de Wall et al. 2004; SAG 2020). The Cabo de Gata-Níjar (Spain) geopark in continental Europe is associated with the Alpine orogen through the extensional collapse-uplift mechanism of the Carboneras fault zone in Spain (Rutter et al. 2012; Scotney et al. 2000). The volcanic theme of this geopark displays late Miocene volcanism beginning in approximately 11 or 7.5 Ma (Scotney et al. 2000; Martin et al. 2003; CVG 2020). The Lesvos Geopark in Greece also contains volcanic remnants of calderas (Lepetymnos, Vatous, and Agra), domes (Mesotopos), and columnar lava (Anemotia) that are linked to Early Miocene (21.5 to 16.5 Ma) volcanic activity (Zouros 2005; LG 2020). These volcanic activities are considered part of the calc-alkaline volcanism domain in the Aegean–Western Anatolia Volcanic Belt above the Hellenic subduction zone (Chakrabarti et al. 2012; Dilek 2006; Innocenti et al. 2005; Zouros 2005). The zone formed due to the accumulation and subduction stages of the Alpine orogeny in the Miocene–Pliocene along the Hellenic arc (Mountrakis 2006) and due to extensional basin development in the Neogene in the Aegean region (Pe-Piper et al. 2019). Relatively younger volcanic themes that resulted from the uplift of the Alps (Alpine orogeny) and the related faulting can be seen in Monts d’Ardèche (France). The volcanism themes of Strombolic craters, domes, maars, dikes and basalt columns are part of the landscape in this geopark. The first phase of volcanism present at Monts d’Ardèche began 12 Ma (Miocene), and the last volcanic episode led to the formation of craters between 12 and 40 ka years ago, in the Pleistocene (MAG 2020).

The only active volcanic terrain in continental Europe is located in the Vulkaneifel Geopark (Germany), where the most recent maar-type geomorphosite (Ulmener Maar) dates to 10,970 years ago and was activated by glacial unloading (Nowell et al. 2006). The south eastern passage to continental Europe is Anatolia (Anatolian Peninsula, Anatolian Plateau, or Asia Minor), where the Kula Geopark (Turkey) is located in the western sector (Aegean Region). The geopark contains basaltic columns, lava flows, and maars from volcanic eruptions dating from  $1.94 \pm 0.16$  Ma to  $4 \pm 2$  ka (Şen et al. 2019). These volcanic themes are part of the Neogene extensional basin (Moores and Fairbridge 1997; Chamot-Rooke et al. 2005) in the Aegean region and formed in association with the Alpine orogenic belt (Moores and Fairbridge 1997; Ziegler and Roure 1999). The Alpine orogeny was initiated by the convergence of Africa and Eurasia (De Graciansky et al. 2011). The collision stage of this orogeny and the retreat of the oceanic slab southward are linked to the widespread arc

volcanism (Şen et al. 2019) known as the Aegean–Western Anatolia Volcanic belt, which extends from the Rhodope Massif–Thrace through the Central Aegean Sea and Western Anatolia (Innocenti et al. 2005).

The most recently active volcanic terrains among the European geopark themes are found in Macaronesia, along the westernmost and south-westernmost fronts of the Atlantic Ocean in Mediterranean Europe. The Canary (Spain) and Azores (Portugal) archipelagos are part of Macaronesia. The Canary archipelago consists of the El Hierro and Lanzarote-Chinijo Islands Geoparks, where a shield volcano (2012 latest eruption date) and pyroclastic cones (1824 latest eruption date), respectively, are found. The Azores archipelago contains the Azores Geopark. This geopark contains several stratovolcanoes, one of which, Terceira, erupted in 1998, representing the most recent event. The Canary archipelago and its geoparks occur in an intraplate hotspot zone (Carracedo et al. 1998). The Azores archipelago and its geoparks occur in the adjoining zone of the Mid-Atlantic Ridge and the Gloria fault, which is a segment of the Azores–Gibraltar fault (Verzhbitskii et al. 2010). In the European Arctic region, along the northernmost front of Europe, the Reykjanes and Katla Geoparks in Iceland formed on the Mid-Atlantic Ridge and represent volcanic fissures comprising lava flows (with the latest eruption date recorded in 1830) and volcanic fissures represented by a stratovolcano (with the latest eruption dates recorded in 2011 and 2010), respectively.

The oldest volcanic themes in the EGN are part of ancient orogenesis (Hercynian, Avalonian-Cadomian, and Caledonian) and occur in continental and Atlantic Europe. They encompass 12% of the entire list of EGN (2020). The geoparks in continental Europe date from Devonian to Permian times. The sites in Atlantic Europe date from Precambrian and Cambrian to Devonian times. The extinct volcanic themes in the EGN formed during the (pre-)Alpine orogeny or in extensional basins related to the Alpine orogeny. These volcanic activities occurred in continental Europe, except for Cyprus Island, and comprise 11% of the EGN list. They date from Mesozoic and Oligocene to Pleistocene times. The active volcanic themes in the EGN reflect different geologic settings. The geoparks related to the extensional basin of the Alpine orogeny occur in the south-eastern passage of continental Europe (Anatolia), with the exception of the Vulkaneifel Geopark (Germany). Macaronesia and the European Arctic region, located far from continental Europe, display different volcanic plumbing mechanism(s) related to a hotspot zone in the Atlantic Ocean, the Mid-Atlantic Ridge or the seismic Gloria fault. These geoparks comprise 9% of EGN list and date from the Holocene to present; however, present volcanic themes are only found along the Atlantic front of Europe.

To summarize, the youngest activity in continental Europe is observed only at the Vulkaneifel Geopark (Germany), and this activity dates to 10,970 years ago. The Kula Geopark, which is on the EGN list, is located in Anatolia, but its volcanism dates to  $4\pm 2$  ka. However, Nemrut volcano, a proposed geopark, exhibits the most recent volcanism, with historical events that occurred in 1441–1597 AD (Şerefhan 1597; Karakhanian et al. 2002; Aydar et al. 2003) at the passage to continental Europe (Anatolia), and this proposed geopark is also a Ramsar site (Ramsar 2019) that includes vulnerable and endangered species (*M. fusca* and endemic plants) (Seven et al. 2019). Additionally, the volcano represents a distinctive cultural landscape with mythical origins (Şerefhan 1597; Karaoğlu and Kılıç 2017) and touristic spots. It also has a steep topography stimulating aesthetic perceptions. Therefore, Nemrut volcano has remarkable value due to its unique geographic-geologic setting along with its biodiversity and cultural values, and this location can be considered a geopark and a geoheritage site.

**Supplementary Information** The online version contains supplementary material available at <https://doi.org/10.1007/s12371-021-00593-5>.

**Acknowledgements** We are grateful to editor, Dr. Kevin Page, and an anonymous reviewer for their constructive comments and suggestions. Thanks are due to Research Assistant Ümit Buğrahan Özcan (Bitlis Eren University, Turkey) for helping to take photos of the geosites. We also thank Instructor Oktay Subaşı (Bitlis Eren University, Turkey) for providing the panoramic views of the Nemrut caldera and Geophysical Engineer Yusuf Mahsereci (AFAD, Bitlis, Turkey) for his help during the field survey.

## References

- AA (2015) Anadolu Agency. Nemrut's camels resisting time. <https://www.hurriyetdailynews.com/nemruts-camels%2D%2Dresisting-time%2D%2D90742>. Accessed 09 Aug 2020
- Aghtamar Church (2020) <https://www.akdamarchurch.gov.tr/>. Accessed 09 Aug 2020
- Akbulut G (2011) A Suggested Geopark Site: Gypsum Karst Topography between Sivas-Zara. In: Efe R, Öztürk M, Atalay İ (eds) Natural Environment and Culture in the Mediterranean Region II, 1st edn. Cambridge Scholars Publishing, pp 137–147
- Akbulut G (2014) Volcano Tourism in Turkey. In: Erfurt-Cooper P (ed) Volcanic Tourist Destinations. Springer, Berlin Heidelberg, Berlin, Heidelberg, pp 89–102
- Akbulut G, Gülüm K (2012) Suggested Geopark Site: Cappadocia. *J Balk Ecol* 15:415–426
- Ateş HÇ, Ateş Y (2019) Geotourism and rural tourism synergy for sustainable development—Marçik Valley Case—Tunceli, Turkey. *Geoheritage* 11:207–215. <https://doi.org/10.1007/s12371-018-0312-1>
- Aydar E, Gourgaud A, Ulusoy İ et al (2003) Morphological analysis of active Mount Nemrut stratovolcano, eastern Turkey: evidences and possible impact areas of future eruption. *J Volcanol Geotherm Res* 123:301–312. [https://doi.org/10.1016/S0377-0273\(03\)00002-7](https://doi.org/10.1016/S0377-0273(03)00002-7)

- Balázs A, Matenco L, Magyar I, Horváth F, Cloetingh SAPL (2016) The link between tectonics and sedimentation in back-arc basins: New genetic constraints from the analysis of the Pannonian Basin. *Tectonics* 35(6):1526–1559. <https://doi.org/10.1002/2015TC004109>
- Balen D, Petrinc Z (2014) Development of columnar jointing in albite rhyolite in a rapidly cooling volcanic environment (Rupnica, Papuk Geopark, Croatia). *Terra Nova* 26(2):102–110. <https://doi.org/10.1111/ter.12075>
- BBG (2020) Bakony-Balaton Geopark. <http://www.geopark.hu/en/home/bakony-balaton-geopark/geological-heritage>. Accessed 04 March 2020
- BirdLife International (2020) Species factsheet: *Melanitta fusca*. <http://datazone.birdlife.org/species/factsheet/velvet-scooter-melanitta-fusca>. Accessed 09 Aug 2020
- Boivin P, Thouret J-C (2014) The Volcanic Chaîne des Puys: a unique collection of simple and compound monogenetic edifices. In: Fort M, André MF (eds) *Landscapes and Landforms of France*, pp 81–91
- Bozkurt E (2001) Neotectonics of Turkey – a synthesis. *Geodin Acta* 14: 3–30. <https://doi.org/10.1080/0985311.2001.11432432>
- BPG 2020 Bohemian Paradise Geopark. <http://www.geoparkceskyraj.cz/en/>. Accessed 30 May 2020
- Brilha J (2016) Inventory and quantitative assessment of geosites and geodiversity sites: a review. *Geoheritage* 8:119–134. <https://doi.org/10.1007/s12371-014-0139-3>
- Brilha J (2018) Geoheritage: inventories and evaluation. In: Emmanuel R, Brilha J (eds) *Geoheritage: Assessment, Protection, and Management*. Elsevier, pp 69–85
- BUGG (2020) Beaujolais Unesco Global Geopark. <http://www.unesco.org/new/en/natural-sciences/environment/earth-sciences/unesco-global-geoparks/list-of-unesco-global-geoparks/france/beaujolais/>. Accessed 23 May 2020
- Carracedo JC, Day S, Guillou H, Badiola ER, Canas JA, Torrado FP (1998) Hotspot volcanism close to a passive continental margin: the Canary Islands. *Geol Mag* 135(5):591–604. <https://doi.org/10.1017/S0016756898001447>
- Çetiner ZS, Ertekin C, Yiğitbaş E (2018) Evaluating scientific value of geodiversity for natural protected sites: the Biga Peninsula, Northwestern Turkey. *Geoheritage* 10:49–65. <https://doi.org/10.1007/s12371-017-0218-3>
- CGIAR–CSI GeoPortal (2012) SRTM 90m DEM digital elevation database. <http://srtm.csi.cgiar.org/>. Accessed 19 May 2019
- Chakrabarti R, Basu AR, Ghatak A (2012) Chemical geodynamics of western Anatolia. *Int Geol Rev* 54(2):227–248. <https://doi.org/10.1080/00206814.2010.543787>
- Chamot-Rooke N, Rangin C, Le Pichon X (2005) DOTMED (Deep Offshore Tectonics of the Mediterranean): A Synthesis of deep marine data in the Eastern Mediterranean. *Mémoires de la Société géologique de France* 177 <http://www.geologie.ens.fr/spiplabocnrs/spip.php?rubrique67>
- Chen A, Lu Y, Ng YCY (2015) *The principles of geotourism*. Springer, Heidelberg
- Çiftçi Y, Güngör Y (2016) Proposals for the standard presentation of elements of natural and cultural heritage within the scope of geopark projects. *Bull Miner Res Explor* 0:223–238. <https://doi.org/10.19111/bmre.80846>
- Çıttroğlu HK, Işık S, Pulat O (2017) Utilizing the geological diversity for sustainable regional development, a case study-Zonguldak (NW Turkey). *Geoheritage* 9:211–223. <https://doi.org/10.1007/s12371-016-0196-x>
- Çubukçu HE (2008) Petrologic evolution of Nemrut Stratovolcano (Türkiye): peralkaline magmatism in a collisional domain. PhD Thesis, Hacettepe University, Turkey and Université Blaise Pascal, France
- Çubukçu HE, Ulusoy İ, Aydar E et al (2012) Mt. Nemrut volcano (Eastern Turkey): temporal petrological evolution. *J Volcanol Geotherm Res* 209–210:33–60. <https://doi.org/10.1016/j.jvolgeores.2011.08.005>
- CVG (2020) La Casa de los Volcanes Geoenvironmental guide Regional Ministry of Environment <http://www.juntadeandalucia.es/medioambiente/servtc5/ventana/mostrarFicha.do?idEquipamiento=160430&lg=EN>. Accessed 12 March 2020
- DAKA (2016) Nemrut Krater Gölü ve Çevresinin Uluslararası Jeopark Ağına Katılımı için Gerekli Fizibilite Çalışmaları (in Turkish). Bitlis De Graciansky PC, Roberts DG, Tricart P (2011) The Alps: Present Day Structure. In *Developments in Earth Surface Processes* 14, Elsevier, pp 29–53. [https://doi.org/10.1016/S0928-2025\(11\)14002-X](https://doi.org/10.1016/S0928-2025(11)14002-X)
- de Lima FF, Brilha JB, Salamuni E (2010) Inventorying geological heritage in large territories: a methodological proposal applied to Brazil. *Geoheritage* 2:91–99. <https://doi.org/10.1007/s12371-010-0014-9>
- de Wall H, Kontny A, Vahle C (2004) Magnetic susceptibility zonation of the melilititic Riedheim dyke (Hegau volcanic field, Germany): evidence for multiple magma pulses? *J Volcanol Geotherm Res* 131(1–2):143–163. [https://doi.org/10.1016/S0377-0273\(03\)00360-3](https://doi.org/10.1016/S0377-0273(03)00360-3)
- Dhont D, Chorowicz J (2006) Review of the neotectonics of the Eastern Turkish–Armenian Plateau by geomorphic analysis of digital elevation model imagery. *Int J Earth Sci* 95:34–49. <https://doi.org/10.1007/s00531-005-0020-3>
- Dilek Y (2006) Collision tectonics of the Mediterranean region: causes and consequences. *Special Papers-Geological Society of America* 409:1–13. [https://doi.org/10.1130/2006.2409\(01\)](https://doi.org/10.1130/2006.2409(01))
- Dingwall P, Weighell T, Badman T (2005) *Geological world heritage: a global framework*
- Doğan U, Şenkul Ç, Yeşilyurt S (2019) First Paleo-Fairy Chimney Findings in the Cappadocia Region, Turkey: a Possible Geomorphosite. *Geoheritage* 11:653–664. <https://doi.org/10.1007/s12371-018-0320-1>
- Dölek İ, Şaroğlu F (2017) Geosites to be used in terms of geotourism in Muş province and its surroundings. *Fırat Üniversitesi Sosyal Bilimler Dergisi* 27:1–16. <https://doi.org/10.18069/firsbed.346467>
- Economicshelp (2020) Real GDP Per Capita. <https://www.economicshelp.org/blog/glossary/real-gdp-capita/>. Accessed 26 July 2020
- EGN (2020) European Geoparks Network. <http://www.europeangeoparks.org/>. Accessed 29 Jan 2020
- Ekinci R (2018) Bitlis ve Yakın Çevresinin Afet Risk Analizi. Master thesis, Graduate School of Natural and Applied Sciences, Bitlis Eren University, Turkey
- Ekinci YL, Büyüksaraç A, Bektaş Ö, Ertekin C (2020a) Geophysical Investigation of Mount Nemrut Stratovolcano (Bitlis, Eastern Turkey) through aeromagnetic anomaly analyses. *Pure Appl Geophys* 177:3243–3264. <https://doi.org/10.1007/s00024-020-02432-0>
- Ekinci R, Büyüksaraç A, Ekinci YL, Işık E (2020b) Bitlis İlinin Doğal Afet Çeşitliliğinin Değerlendirilmesi. *Doğal Afetler ve Çevre Dergisi* 6:1–11. <https://doi.org/10.21324/dacd.535189>
- Emre Ö, Duman TY, Özalp S, et al (2013) Active fault map of Turkey with an explanatory text (1:1,250,000 scale). The General Directorate of Mineral Research and Exploration, Special Publication Series-30. Ankara, Turkey
- Emre Ö, Duman TY, Özalp S et al (2018) Active fault database of Turkey. *Bull Earthq Eng* 16:3229–3275. <https://doi.org/10.1007/s10518-016-0041-2>
- Encyclopædia Britannica (2020a) <https://www.britannica.com/place/Urartu>. Accessed 29 Jan 2020
- Encyclopædia Britannica (2020b) <https://www.britannica.com/biography/Tukulti-Ninurta-I>. Accessed 29 Jan 2020
- Encyclopædia Britannica (2020c) <https://www.britannica.com/biography/Tukulti-Ninurta-II>. Accessed 29 Jan 2020
- Erturaç MK, Okur H, Ersoy B (2017) Göllüdağ Volkanik Kompleksi İçerisinde Kültürel ve Jeolojik Miras Ögeleri. *Türkiye Jeol Bülteni / Geol Bull Turkey* 60:17–34. <https://doi.org/10.25288/tjb.297803>

- Kef Fortress (2020) <https://www.urartians.com/alticerik/48/kef-fortress-haldiei-uru.html>. Accessed 09 Aug 2020
- Frahm E (2020) Variation in Nemrut Dağ obsidian at Pre-Pottery Neolithic to Late Bronze Age sites (or: all that's Nemrut Dağ obsidian isn't the Sicaksu source). *J Archaeol Sci Rep* 32:102438. <https://doi.org/10.1016/j.jasrep.2020.102438>
- Frödin J (1937) La Morphologie De La Turquie Sud-Est. *Geogr Ann* 19: 1–29. <https://doi.org/10.1080/20014422.1937.11880622>
- Gadjimuradov I, Schmoekkel R (2005) Das Geheimnis des anatolischen Meeres: der Garten Eden, die Sintflut und die Hölle; der rebellische Vulkan und die ältesten Mythen der Welt. BoD–Books on Demand
- GB (2020) Geopark Beaujolais. <https://www.geopark-beaujolais.com/en/geologie.html>. Accessed 14 April 2020
- GMC (1979) Geological map of Cyprus 1:250,000 scaled, Geological Survey Department. <https://esdac.jrc.ec.europa.eu/content/geological-map-cyprus>. Accessed 12 June 2020
- Gray M (2013) *Geodiversity: valuing and conserving abiotic nature*, 2nd edn. Wiley-Blackwell
- GSL (2020) The Geological Society of London. <https://www.geol Soc.org.uk/Plate-Tectonics/Chap4-Plate-Tectonics-of-the-UK/Caledonian-Orogeny>. Accessed 19 February 2020
- GSMA (2020a) Global System for Mobile Communications. <https://www.gsma.com/coverage/#534>. Accessed 31 July 2020
- GSMA (2020b) Global System for Mobile Communications. <https://www.gsma.com/coverage/#532>. Accessed 31 July 2020
- GSMA (2020c) Global System for Mobile Communications. <https://www.gsma.com/coverage/#514>. Accessed 31 July 2020
- Güngör Y, İskenderoğlu L, Azaz D, Güngör B (2012) Geopark inventory study of Levent Valley, Akçadağ-Malatya. In: *International Multidisciplinary Scientific GeoConference : SGEM : Surveying Geology & Mining Ecology Management*. Sofia, pp 125–135
- Gürbüz O (1995) Turizm Coğrafyası Açısından Nemrut Kalderası (in Turkish). *Türk Coğrafya Dergisi* 30:255–265 <https://dergipark.org.tr/en/pub/tcd/issue/21257/228147>
- Gürer A, Gürer ÖF, Sangu E (2019) Compound geotourism and mine tourism potentiality of Soma region, Turkey. *Arab J Geosci* 12:1–14. <https://doi.org/10.1007/s12517-019-4927-6>
- Gürler G, Derman AS (2012) Mut Miyosen Havzası" Öneri Jeopark Alanının Jeolojik Miras Açısından Değerlendirilmesi (in Turkish). Ankara
- Gürler G, Uğuz MF, Öztan NS (2013) Karapınar Potansiyel Jeopark Alanı ve Jeoturizm Açısından Değerlendirilmesi (in Turkish). Ankara
- GVA (2020a) Geopark Vis Arcipelago. <https://geopark-vis.com/en/geology/geology-of-the-vis-archipelago>. Accessed 2 June 2020
- GVA (2020b) Geopark Vis Arcipelago. <http://www.unesco.org/new/en/natural-sciences/environment/earth-sciences/unesco-global-geoparks/list-of-unesco-global-geoparks/croatia/vis-archipelago/>. Accessed 2 June 2020
- Hatipoğlu M (2010) Gem-quality diaspore crystals as an important element of the geoheritage of Turkey. *Geoheritage* 2:1–13. <https://doi.org/10.1007/s12371-009-0008-7>
- Innocenti F, Agostini S, Di Vincenzo G, Doglioni C, Manetti P, Savaşçın MY, Tonarini S (2005) Neogene and Quaternary volcanism in Western Anatolia: magma sources and geodynamic evolution. *Mar Geol* 221(1–4):397–421. <https://doi.org/10.1016/j.margeo.2005.03.016>
- Jemirko (2014) Jemirko Türkiye Jeolojik Miras Envanteri. <http://www.jemirko.org.tr/download/envanter-listesi-detayli/>. Accessed 24 Sep 2018
- Jemirko (2018) Jeositler <https://www.jemirko.org.tr/download/jeositler/> Accessed 24 Sep 2018
- Karahan F, Kopar İ, Orhan T, Çakır E (2011) The geopark potential of Tortum Valley (Erzurum-Turkey) and its surroundings. In: Efe R, Öztürk M, Atalay İ (eds) *Natural Environment and Culture in the Mediterranean Region II*, 1st edn. Cambridge Scholars Publishing, pp 395–406
- Karakhanian A, Djrashian R, Trifonov V et al (2002) Holocene-historical volcanism and active faults as natural risk factors for Armenia and adjacent countries. *J Volcanol Geotherm Res* 113: 319–344. [https://doi.org/10.1016/S0377-0273\(01\)00264-5](https://doi.org/10.1016/S0377-0273(01)00264-5)
- Karaoğlu Ö, Kılıç S (2017) Nemrut Volkanı ve Kral Nemrut'un Efsaesi (in Turkish). *Mavi Gezegen*:29–37
- Karaoğlu Ö, Özdemir Y, Tolluoğlu AÜ et al (2005) Stratigraphy of the volcanic products around Nemrut caldera: implications for reconstruction of the caldera formation. *Turk J Earth Sci* 14:123–143
- Kaygılı S, Aksoy E (2017) Kovancılar (Elazığ, Türkiye) Jeositi: Nummulites'li seviyeler ve Antiklinal (in Turkish). *Fırat Üniversitesi Mühendislik Bilim Derg* 29:293–299
- Kaygılı S, Avcı N, Aksoy E (2017) Paleontolojik Bir Jeosit Örneği: Hasanağa Deresi, Akçadağ, Malatya (in Turkish). *Türkiye Jeol Bülteni / Geol Bull Turkey* 60:93–106. <https://doi.org/10.25288/tjb.297840>
- Kaygılı S, Sinanoğlu D, Aksoy E, Şaşmaz A (2018) Geoturizm: some examples from Turkey. *Bull Univ Dnipro Geol Geogr* 26:79–87. <https://doi.org/10.15421/111809>
- Kazancı N (2012) Geological background and three vulnerable geosites of the Kızılcahamam-Çamlıdere Geopark Project in Ankara, Turkey. *Geoheritage* 4:249–261. <https://doi.org/10.1007/s12371-012-0064-2>
- Kazancı N, Gürbüz A (2014) Jeolojik Miras Nitelikli Türkiye Doğal Taşları (in Turkish). *Türkiye Jeol Bülteni / Geol Bull Turkey* 57: 19–44. <https://doi.org/10.25288/tjb.298752>
- Kazancı N, Suludere Y, Mülazımoğlu NS, et al (2007) Orta Anadolu'daki Milli Parklar ve Yakın Civarındaki Jeosit ve Jeomiras Ögelerinin Belirlenmesi ve Değerlendirilmesi (in Turkish). Ankara
- Kızılmaz İ (2014) The Monuments of Urartian Period in Van and Bitlis and excavations in the region. Master Thesis, Fırat University. Turkey
- KKG (2020) Karavanke/Karawanken Geopark. <https://www.geopark-karawanken.at/en/home.html>. Accessed 14 March 2020
- Koçyiğit A, Yılmaz A, Adamia S, Kuloshvili S (2001) Neotectonics of East Anatolian Plateau (Turkey) and Lesser Caucasus: implication for transition from thrusting to strike-slip faulting. *Geodin Acta* 14: 177–195. <https://doi.org/10.1080/09853111.2001.11432443>
- KOERI (2021) Boğaziçi University Kandilli Observatory and Earthquake Research Institute. <http://www.koeri.boun.edu.tr/sismo/2/en/>. Accessed 03 January 2021
- Kopar İ, Çakır Ç (2014) Tortum Gölü-Tortum Boğaz Vadisi ve Yakın Çevresinin (Uzundere-Erzurum ve Yusufeli-Artvin) Serrano ve Ruiz-Flaño Yöntemiyle Jeoçeşitlilik Derecesinin Belirlenmesi (in Turkish). *Coğrafya Derg* 27:46–66
- Koroğlu F, Kandemir R (2019) Vulnerable Geosites of Çayırbağı-Çalköy (Düzköy-Trabzon) in the Eastern Black Sea Region of NE Turkey and Their Geotourism Potential. *Geoheritage*:1–11. <https://doi.org/10.1007/s12371-019-00358-1>
- Kralj P (2012) Facies architecture of the Upper Oligocene submarine Smrekovec stratovolcano, Northern Slovenia. *J Volcanol Geotherm Res* 247:122–138. <https://doi.org/10.1016/j.jvolgeores.2012.07.016>
- Kurttaş T, Tezcan L (2017) Nemrut Kaldera Göllerinin Su Kaynakları Potansiyeli (in Turkish). *Süleyman Demirel Üniversitesi Fen Bilim Enstitüsü Derg* 22:823. <https://doi.org/10.19113/sdufbed.93985>
- Lawrence DJD, Vye CL, Young B (2004) *Durham Geodiversity Audit*. Durham: Durham County Council, The British Geological Survey. <https://www.durham.gov.uk/media/3683/County-Durham-GeodiversityAudit/pdf/CountyDurhamGeodiversityAudit.pdf?m=636735641814470000>
- Lebedev VA, Sharkov EV, Keskin M, Oyan V (2010) Geochronology of Late Cenozoic volcanism in the area of Van Lake, Turkey: an example of development dynamics for magmatic processes. *Dokl*

- Earth Sc 433:1031–1037. <https://doi.org/10.1134/S1028334X1008009X>
- Lebedev VA, Sharkov EV, Ünal E, Keskin M (2016) Late pleistocene Tendürek volcano (Eastern Anatolia, Turkey): I. Geochronology and petrographic characteristics of igneous rocks. *Petrology* 24(2): 127–152. <https://doi.org/10.1134/S0869591116020041>
- LG (2020) Lesvos Geopark. <http://www.lesvosgeopark.gr/volcanos/?lang=en>. Accessed 06 March 2020
- Linnemann U, Gerdes A, Drost K, Buschmann B (2007) The continuum between Cadomian orogenesis and opening of the Rheic Ocean: Constraints from LA-ICP-MS U-Pb zircon dating and analysis of plate-tectonic setting (Saxo-Thuringian zone, northeastern Bohemian Massif, Germany). In: Linnemann U, Damian Nance R, Kraft P, Zulauf G (eds) *The evolution of the Rheic Ocean: from Avalonian-Cadomian active margin to Alleghenian-Variscan collision*, 423, pp 61–96, Geological Society of America. [https://doi.org/10.1130/2007.2423\(03\)](https://doi.org/10.1130/2007.2423(03))
- Lozić S, Krklec K, Perica D (2012) Typology of Vis Island based on influence of geological, geomorphological and pedological characteristics on natural and cultural landscape. *NAŠE MORE: znanstveno-stručni časopis za more i pomorstvo* 59(1-2):82–91 <https://hrcak.srce.hr/83544>. Accessed 2 June 2020
- MAF (2020) Ministry of Agriculture and Forestry. <https://www.tarimorman.gov.tr/DKMP/Belgeler/Korunan%20Alanlar%20Listesi/3-TAB%C4%B0AT%20ANITLARI.pdf>. Accessed 09 Aug 2020
- MAG (2020) Monts d'Ardèche Geopark. [http://www.geopark-monts-ardeche.fr/images/phocadownload/2018/depliant-en\\_031.pdf](http://www.geopark-monts-ardeche.fr/images/phocadownload/2018/depliant-en_031.pdf). Accessed 14 April 2020
- Martín JM, Braga JC, Betzler C (2003) Late Neogene-recent uplift of the Cabo de Gata volcanic province, Almería, SE Spain. *Geomo* 50(1): 27–42. [https://doi.org/10.1016/S0169-555X\(02\)00206-4](https://doi.org/10.1016/S0169-555X(02)00206-4)
- MBS (2020) Mevzuat Bilgi Sistemi (in Turkish). <http://www.mevzuat.gov.tr/MevzuatMetin/1.5.2863-20131008.pdf>. Accessed 09 Aug 2020
- Moores EM, Fairbridge RW (eds) (1997) *Encyclopedia of European and Asian Regional Geology Encyclopedia of Earth Sciences Book Series*, Chapman & Hall, pp 825. In: Hadi M, Mosaddegh H, Abbassi N (2016) Microfacies and biofabric of nummulite accumulations (Bank) from the Eocene deposits of Western Alborz (NW Iran). *J Afr Earth Sci* 124:216–233. <https://doi.org/10.1016/j.jafrearsci.2016.09.012>
- Morag N, Haviv I, Katzir Y (2016) From ocean depths to mountain tops: Uplift of the Troodos ophiolite (Cyprus) constrained by low-temperature thermochronology and geomorphic analysis. *Tectonics* 35(3):622–637. <https://doi.org/10.1002/2015TC004069>
- Mountrakis D (2006) Tertiary and Quaternary tectonics of Greece. In: Dilek Y, Pavlides S (eds) *Postcollisional tectonics and magmatism in the Mediterranean region and Asia*, GSA Special Papers-Geological Society of America 409, pp 125–136. [https://doi.org/10.1130/2006.2409\(07\)](https://doi.org/10.1130/2006.2409(07))
- MTA (1964) The General Directorate of Mineral Research and Exploration. Geological map of Turkey (1:500,000 scale). Ankara, Turkey
- Murphy JB, Nance RD, Keppie JD, Dostal J (2019) Role of Avalonia in the development of tectonic paradigms. *Geol Soc Lond, Spec Publ* 470(1):265–287. <https://doi.org/10.1144/SP470.12>
- NASA EarthData (2020) <https://search.earthdata.nasa.gov/search>. Accessed 21 December 2020
- Nizamettin K, Şaroğlu F, Suludere Y (2015) Geological Heritage and Framework List of The Geosites In Turkey. *Bull Miner Res Explor* 151:259–268. <https://doi.org/10.19111/bmre.39701>
- NOAA (2020) National Oceanic and Atmospheric Administration. National Geophysical Data Center / World Data Service (NGDC/WDS): Significant Volcanic Eruptions Database. National Geophysical Data Center, NOAA. doi:<https://doi.org/10.7289/V5JW8BSH>
- Notsu K, Fujitani T, Ui T et al (1995) Geochemical features of collision-related volcanic rocks in central and eastern Anatolia, Turkey. *J Volcanol Geotherm Res* 64:171–191. [https://doi.org/10.1016/0377-0273\(94\)00077-T](https://doi.org/10.1016/0377-0273(94)00077-T)
- Nowell DAG, Jones MC, Pyle DM (2006) Episodic Quaternary volcanism in France and Germany. *J Quat Sci* 21:645–675. <https://doi.org/10.1002/jqs.1005>
- NP (2020) The North P A.O.N.B. European Geopark–UK. <https://www.northpennines.org.uk/whats-special/geology-and-landscape/>. Accessed 03 March 2020
- OpenStreetMap. <https://www.openstreetmap.org/export#map=10/38.6255/42.2493>. Accessed 27 Oct 2019
- Özdemir Y, Güleç N (2014) Geological and geochemical evolution of the Quaternary Süphan Stratovolcano, Eastern Anatolia, Turkey: evidence for the lithosphere–asthenosphere interaction in post-collisional volcanism. *J Petrol* 55(1):37–62. <https://doi.org/10.1093/petrology/egt060>
- Özdemir Y, Karaoğlu Ö, Tolluoğlu AÜ, Güleç N (2006) Volcanostratigraphy and petrogenesis of the Nemrut stratovolcano (East Anatolian High Plateau): The most recent post-collisional volcanism in Turkey. *Chem Geol* 226:189–211. <https://doi.org/10.1016/j.chemgeo.2005.09.020>
- Öziş Ü (2015) Water works through four millenia in Turkey. *Environ Process* 2:559–573. <https://doi.org/10.1007/s40710-015-0085-3>
- Özsoy M (2010) Mt. Nemrud Caldera. In: Evelpidou N, Figueiredo T, Mauro F, Tecim V, Vassilopoulos A (eds) *Natural Heritage from East to West*, pp 353–359
- Pamić J (1991) Gornjokredne bazaltoidne i piroklastične stijene iz voćinske vulkanske mase na Papuku (Slavonija, sj. Hrvatska) (Upper Cretaceous basaltoid and pyroclastic rocks from the Voćin volcanic mass on the Papuk Mt. (Slavonija, Northern Croatia)). *Geol Vjesn* (44):161–172 [http://31.147.204.208/clanci/1991\\_Pamic\\_1009%20\(2\).pdf](http://31.147.204.208/clanci/1991_Pamic_1009%20(2).pdf)
- Pánisová J, Balázs A, Zalai Z, Bielik M, Horváth F, Harangi S, Schmidt S, Götze HJ (2018) Intraplate volcanism in the Danube Basin of NW Hungary: 3D geophysical modelling of the Late Miocene Pásztori volcano. *Int J Earth Sci (Geol Rundsch)* 107(5):1713–1730. <https://doi.org/10.1007/s00531-017-1567-5>
- Pawlewicz MJ, Steinshouer DW, Gautier DL (1997) Map showing geology, oil and gas fields, and geologic provinces of Europe including Turkey: U.S. Geological Survey Open-File Report 97-470-I
- Pe-Piper G, Piper DJ, Zouros N, Anastasakis G (2019) Age, stratigraphy, sedimentology and tectonic setting of the Sigrí Pyroclastic Formation and its fossil forests, Early Miocene, Lesbos, Greece. *Basin Res* 31(6):1178–1197. <https://doi.org/10.1111/bre.12365>
- PGG (2020) Papuk Geopark. <https://pp-papuk.hr/papuk-unesco-geopark/?lang=en>. Accessed 05 June 2020
- Ramsar (2019) Ramsar sites information service. <https://rsis.ramsar.org/ris/2145>. Accessed 19 May 2019
- Ring U, Pantazides H (2019) The Uplift of the Troodos Massif, Cyprus. *Tectonics* 38(8):3124–3139. <https://doi.org/10.1029/2019TC005514>
- Robin AK, Mouralis D, Akköprü E et al (2016) Identification and characterization of two new obsidian sub-sources in the Nemrut volcano (Eastern Anatolia, Turkey): The Sicaksu and Kayacık obsidian. *J Archaeol Sci Rep* 9:705–717. <https://doi.org/10.1016/j.jasrep.2016.08.048>
- Ruban DA (2010) Quantification of geodiversity and its loss. *Proceedings of the Geologists' Association. The Geologists' Association*, In, pp 326–333
- Rutter EH, Faulkner DR, Burgess R (2012) Structure and geological history of the Carboneras Fault Zone, SE Spain: Part of a stretching transform fault system. *J Struct Geol* 45:68–86. <https://doi.org/10.1016/j.jsg.2012.08.009>

- Rypl J, Kirchner K, Dvořáčková S (2016) Geomorphological Inventory as a Tool for Proclaiming Geomorphosite (a Case Study of Mt. Myslívna in the Novohradské hory Mts.—Czech Republic). *Geoheritage* 8:393–400. <https://doi.org/10.1007/s12371-015-0169-5>
- SAG (2020) Swabian Albs Geopark. <https://www.geopark-alb.de/en/geopark-erleben/geologische-highlights.php>. Accessed 17 March 2020
- SAGA GIS (2020) SAGA System for Automated Geoscientific Analyses (Version 7.9.0. <http://www.saga-gis.org>
- SAYS (2020) Sit Alanları Yönetim Bilgi Sistemi. <https://www.says.gov.tr/savab/#/>. Accessed 09 Aug 2020
- Scotney P, Burgess R, Rutter EH (2000) 40Ar/39Ar age of the Cabo de Gata volcanic series and displacements on the Carboneras fault zone, SE Spain. *J Geol Soc* 157(5):1003–1008. <https://doi.org/10.1144/jgs.157.5.1003>
- Selvaggio I, Magagna A, Giardino M (2016) Understanding The Supervolcano with An Inquiry-Based Approach. In 7th International Conference on Global Geoparks p: 155. [http://www.globalgeopark.org/UploadFiles/2016\\_11\\_2/Abstract\\_Book%20of%20the%207th%20international%20conference%20on%20UNESCO%20Global%20Geoparks.pdf](http://www.globalgeopark.org/UploadFiles/2016_11_2/Abstract_Book%20of%20the%207th%20international%20conference%20on%20UNESCO%20Global%20Geoparks.pdf)
- Şen E, Erturaç MK, Gümüş E (2019) Quaternary monogenetic volcanoes scattered on a horst: the bountiful landscape of Kula. In: Çiner A, Kazancı N (eds) *Kuzucuoğlu C. Landscapes and Landforms of Turkey*, Springer, pp 577–588. [https://doi.org/10.1007/978-3-030-03515-0\\_34](https://doi.org/10.1007/978-3-030-03515-0_34)
- Şerefhan (1597). Şerefname: Kurdish history (translated from Arabic to Turkish by M. Emin Bozarslan). Hasat yayınları 4th ed. (1990).
- Serrano E, Ruiz-Flaño P (2007) Geodiversity. A theoretical and applied concept. *Geogr Helv* 62:140–147. <https://doi.org/10.5194/gh-62-140-2007>
- Seven E, Mironov V, Akın K (2019) A new species of *Eupithecia curtis* (Lepidoptera: Geometridae, Larentiinae) from Turkey. *Zootaxa* 4668:443–447. <https://doi.org/10.11646/zootaxa.4668.3.9>
- SIGVP (2013) Global Volcanism Program. Volcanoes of the World, v. 4.9.0 (04 Jun 2020). In: Venzke E (ed) Smithsonian Institution. <https://doi.org/10.5479/si.GVP.VOTW4-2013> Accessed 29 Jun 2020
- SVG (2020) Sesia-Val Grande Geopark. <http://www.unesco.org/new/en/natural-sciences/environment/earth-sciences/unesco-global-geoparks/list-of-unesco-global-geoparks/italy/sesia-val-grande/>. Accessed 04 March 2020
- TG (2020) Troodos Geopark. <https://www.prettypmap.gr/troodos/geosites/>. Accessed 10 Jun 2020
- TSI (2020) Turkish Statistical Institute. <https://biruni.tuik.gov.tr/ilgosterge/?locale=en>. Accessed 24 July 2020
- TUGG (2020) Troodos Unesco Global Geopark. <http://www.unesco.org/new/en/natural-sciences/environment/earth-sciences/unesco-global-geoparks/list-of-unesco-global-geoparks/cyprus/troodos/>. Accessed 12 June 2020
- Ulrych J, Pešek J, Šte J, Bosák P, Lloyd FE, Von Seckendorff V, Lang M, Novák JK (2006) Permo-Carboniferous volcanism in late Variscan continental basins of the Bohemian Massif (Czech Republic): geochemical characteristic. *Geochemistry* 66(1):37–56. <https://doi.org/10.1016/j.chemer.2004.02.001>
- Ulrych J, Dostal J, Adamovič J, Jelínek E, Špaček P, Hegner E, Balogh K (2011) Recurrent Cenozoic volcanic activity in the Bohemian Massif (Czech Republic). *Lithos* 123(1–4):133–144. <https://doi.org/10.1016/j.lithos.2010.12.008>
- Ulusoy İ (2008) Etude volcano-structurale du volcan Nemrut (Anatolie de l'Est, Turquie) et risques naturels associés. PhD Thesis, Hacettepe University, Turkey and Université Blaise Pascal, France
- Ulusoy İ, Labazuy P, Aydar E et al (2008) Structure of the Nemrut caldera (Eastern Anatolia, Turkey) and associated hydrothermal fluid circulation. *J Volcanol Geotherm Res* 174:269–283. <https://doi.org/10.1016/j.jvolgeores.2008.02.012>
- Ulusoy İ, Çubukçu HE, Aydar E et al (2012) Volcanological evolution and caldera forming eruptions of Mt. Nemrut (Eastern Turkey). *J Volcanol Geotherm Res* 245–246:21–39. <https://doi.org/10.1016/j.jvolgeores.2012.06.031>
- Ulusoy İ, Çubukçu HE, Mouralis D, Aydar E (2019) Nemrut Caldera and Eastern Anatolian Volcanoes: Fire in the Highlands. In: Kuzucuoğlu C, Çiner A, Kazancı N (eds) *Landscapes and Landforms of Turkey*, pp 589–599
- Üner S, Alırız MG, Özsayın E et al (2017) Earthquake Induced Sedimentary Structures (Seismites): Geoconservation and Promotion as Geological Heritage (Lake Van-Turkey). *Geoheritage* 9:133–139. <https://doi.org/10.1007/s12371-016-0186-z>
- Uzun A (2017) Bir Açık Alan Dersliği: Kandıra Kıyıları (Kocaeli, Türkiye) (in Turkish). *Türkiye Jeol Bülteni / Geol Bull Turkey* 60: 117–128. <https://doi.org/10.25288/tjb.297854>
- Verzhbitskii EV, Kononov MV, Byakov AF, Grinberg OV (2010) Specific features of the genesis of the Azores-Gibraltar fault zone (North Atlantic). *Izv., Phys. Solid Earth* 46(10):872–882. <https://doi.org/10.1134/S1069351310100071>
- Vlahović I, Tišljarić J, Velić I, Matičec D (2005) Evolution of the Adriatic Carbonate Platform: Palaeogeography, main events and depositional dynamics. *Palaeogeogr Palaeoclimatol Palaeoecol* 220(3–4):333–360. <https://doi.org/10.1016/j.palaeo.2005.01.011>
- Wood C (2009) World heritage volcanoes a thematic study: a global review of volcanic world heritage properties: present situation, future prospects and management requirements. Gland, Switzerland
- Yığıtbaş E, Elmas A, Sefunç A, Özer N (2004) Major neotectonic features of eastern Marmara region, Turkey: development of the Adapazarı-Karasu corridor and its tectonic significance. *Geol J* 39: 179–198. <https://doi.org/10.1002/gj.962>
- Yılmaz Y, Güner Y, Şaroğlu F (1998) Geology of the quaternary volcanic centres of the east Anatolia. *J Volcanol Geotherm Res* 85:173–210. [https://doi.org/10.1016/S0377-0273\(98\)00055-9](https://doi.org/10.1016/S0377-0273(98)00055-9)
- Ziegler PA, Roure F (1999) Petroleum systems of Alpine-Mediterranean foldbelts and basins. *Geol Soc Lond, Spec Publ* 156(1):517–540. <https://doi.org/10.1144/GSL.SP.1999.156.01.23>
- Zouros N (2005) Assessment, protection, and promotion of geomorphological and geological sites in the Aegean area, Greece. *Géomorphologie: relief, processus, environnement* 11(3):227–234. <https://doi.org/10.4000/geomorphologie.398>
- Zwoliński Z, Najwer A, Giardino M (2018) Methods for assessing geodiversity. In: Emmanuel R, Brilha J (eds) *Geoheritage: Assessment, Protection, and Management*. Elsevier, pp 27–52